BIOMECHANICAL EFFECTS OF POWERED PROTHESIS AND PASSIVE PROSTHESIS

A Dissertation
Presented to
The Academic Faculty

By

Sixu Zhou

In Partial Fulfillment
of the Requirements for the Degree
Master of Science in the
School of Engineering
Department of Mechanical Engineering

Georgia Institute of Technology

May 2022

BIOMECHANICAL EFFECTS OF POWERED PROTHESIS AND PASSIVE PROSTHESIS

Thesis committee:

Dr. Aaron Young
Department of Mechanical Engineering
Georgia Institute of Technology

Dr. Frank Hammond III
Department of Mechanical Engineering
Georgia Institute of Technology

Kinsey Herrin, MSPO, C/LPO, FAAOP
Department of Mechanical Engineering
Georgia Institute of Technology

Date approved: April 29, 2022

ACKNOWLEDGMENTS

I would like to thank the members of my thesis committee for their help in preparation of this work – Dr. Aaron Young for all the grateful advice and support for this research work, Dr. Frank Hammond for directing me and guiding me in the professional field, Kinsey Herrin for supporting me all the time through my study.

Special thanks are due to the friends and colleagues who made this work possible. Krishan Bhakta, Jairo Maldonado-Contreras, Jonathan Camargo and Christoph Nuesslein all guided and directed me into this team, encouraged me and became the invaluable friends of mine.

Special thanks to my lovely wife Stella Ren who sacrificed her music studies to come to Atlanta along with me. I could not achieve where I am right now without her. Thanks to my parent and all other family members for supporting me.

The author gratefully acknowledges the support for this work offered by Congressionally Directed Medical Research Program under grant award numbers GR00011794 and GR10000440. Any views and conclusions contained herein are those of the author, and do not necessarily represent the official positions, express or implied, of the funders.

TABLE OF CONTENTS

Acknowledgments iii

List of Tables vii

List of Figures viii

List of Acronyms x

Summary xi

Chapter 1: Introduction 1

1.1 Background 1

1.2 Prosthesis Prior Art 1

1.2.1 Passive Prosthesis 2

1.2.2 Active Prosthesis 4

1.3 Human Biomechanics 5

1.3.1 Whole Body Angular Momentum 5

1.3.2 Able Body Biomechanics 6

1.4 Motivation 6

Chapter 2: Narrowing Beam Walking Test Balance Study 8

2.1 Overview 8

2.2 Methodology 8
2.2.1 Experimental Devices 8
2.2.2 Experiment Protocol 10
2.2.3 Biomechanics 11
2.3 Results 14
2.3.1 Distance Traveled and Stride Time on NBWT 14
2.3.2 WBAM Comparison Between AB and TF on NBWT 15
2.3.3 IK and WBAM among All MPKs on NBWT 16
2.3.4 WBAM at the Last Gait Cycle on NBWT 17
2.3.5 WBAM at Each Segment of the Beam on NBWT 18
2.3.6 Peak-to-Peak WBAM on NBWT 18
2.4 Discussion 19

Chapter 3: Initial OSL Biomechanics Study 24

3.1 Overview 24
3.2 Methodology 24
3.2.1 Experimental Device 24
3.2.2 Control Paradigm 25
3.2.3 Biological Inspired Scaling Equations 28
3.2.4 Experiment Protocol 29
3.3 Results 30
3.3.1 IK, GRF, ID and JP 30
3.3.2 Energy Expenditure 32

3.3.3 Handrail Usage and Stride Metrics 33
3.4 Discussion 34

Chapter 4: Device Development 36
4.1 Overview 36
4.2 Sit-to-Stand Controller 36
4.3 Graphical User Interface 37
4.4 DENEB Pipeline 38
4.4.1 OpenSim OSL model 38
4.4.2 Model Validation 39

Chapter 5: Iterated Ramp Scaling Walking Study 41
5.1 Methodology 41
5.1.1 Controller Modification 41
5.1.2 Experiment Protocol 43
5.2 Results 43
5.3 Discussion 44

Chapter 6: Discussion and Conclusion 46
6.1 Narrowing Beam Walking Test Balance Study 46
6.2 Iterated Ramp Scaling Walking Study 46
6.3 Limitation and Future Work 47

References 49

LIST OF TABLES

3.1 Open-Source Leg Specs 26

3.2 Handrail Usage 34

3.3 Stride Metrics 35

LIST OF FIGURES

1.1 Transfemoral Prosthesis User 3

2.1 Lower Limb Prosthesis Users on NBWT 9

2.2 Narrowing Beam Walking Test During Experiment 11

2.3 OpenSim Musculoskeletal Model with Prosthesis 12

2.4 Distance Traveled on NBWT 14

2.5 Stride Time on NBWT 15

2.6 Whole Body Angular Momentum Comparison between AB Subject and Unilateral Transfemoral Subject MPK01 on the Narrowing Beam Walking Test 16

2.7 Whole Body Angular Momentum Comparison between AB Subject and Unilateral Transfemoral Subject MPK02 on the Narrowing Beam Walking Test 16

2.8 Inverse kinematics result segmented in gait cycles across all three microprocessor knees 17

2.9 Whole body angular momentum result segmented in gait cycles across all three microprocessor knees 18

2.10 WBAM evaluation at the last gait cycle of the beam 19

2.11 MPK01 WBAM evaluation at each segment of the beam 20

2.12 MPK02 WBAM evaluation at each segment of the beam 21

2.13 WBAM Peak to Peak 22

3.1 Open-Source Leg 25

3.2 AB Knee Biomechanics 28

3.3 Ramp Scaling Controller Protocol 31

3.4 Unilateral Transfemoral Amputee Intact Limb side when wearing Active Prosthesis 32

3.5 Unilateral Transfemoral Amputee Prosthetic Limb side when wearing Active Prosthesis 33

3.6 Energy Expenditure Pie Chart Among Unilateral Transfemoral Amputee Prosthetic Limb Side when Wearing Active and Passive Prosthesis 34

5.1 Knee Prosthetic and Intact Limb Biomechanics with AB Adaptor 44

5.2 Stride Metrics with AB Adaptor 45

LIST OF ACRONYMS

AB Able Body

ABC Activities-specific Balance Confidence

BBS Berg Balance Scale

COM Center of Mass

DOF Degree-of-Freedom

EMG Electromyography

FSM Finite State Machine

FSST Four Square Step Test

GRFs ground reaction forces

ID Inverse Dynamics

IK Inverse Kinematics

IMU Inertial Measurement Units

MPK Microprocessor Prostheic Knees

NBWT Narrowing Beam Walking Test

OSL Open-Source Leg

ROM Range of Motion

SEA Series Elastic Actuators

TF transfemoral

WBAM Whole Body Angular Momentum

SUMMARY

The population of individuals with transfemoral amputation is expected to grow rapidly over the next few decades. The impact of mobility due to lower extremity loss worsens the quality of life of these individuals. One of the most common solutions is to use a lower extremity prosthesis to rehabilitate the locomotion tasks of normal daily living. The first section presented in this thesis study is to evaluate the balance of lower limb prosthesis users on beam walking. Meanwhile, inspired by the biomechanical data of able body locomotion, no state-of-the-art control strategy has been discovered to adapt biomechanics when individuals with a transfemoral amputation walk in different slope contexts while wearing an active knee and ankle prosthesis. Thus, the second section presented in this thesis study is to design a smart midlevel controller to produce the kinematics and kinetics profiles of the active prosthesis users with scaling assistance. All studies used biomechanical information as outcome measures.

Two different types of experiments were performed: one with narrowing beam walking test on three MPKs including Cleg 4.0, RheoKnee and PowerKnee, and another slope walking test on knee-and-ankle active prosthesis. From the balance evaluation experiment, PowerKnee and RheoKnee both exhibited similar performance on the distance traveled on the beam. There is a distinct difference in WBAM regulation as the contact surface area is reduced as the beam becomes narrower. WBAM of the last gait cycle which represented as the falling event shows a higher frontal peak-to-peak values and might be affected by the foot placement. The quantified value when the fall occurs cannot be determined due to limits of testings.

The smart controller takes several iterations to improve the performance of the biomechanical outcomes. Development tools are built and presented to help users better adapt to the device. A concluding able body test is performed to validate knee scaling control, but is not fully validated in application to individuals with transfemoral amputation.

CHAPTER 1
INTRODUCTION

1.1 Background

By 2050, it is estimated that the limb-loss population will reach 3.6 million and 18% will be transfemoral (TF) individuals with transfemoral (TF) amputation [1]. Causes of lower limb amputation are due to disease, and secondary causes include trauma and congenital limb absence [2]. The primary outcome of rehabilitation, ambulation, has been reported to be associated with the level of amputation and the use of prostheses [3]. The quality of life of people with lower extremity amputation is significantly associated with mobility [4]. The loss of a lower limb affect their ambulation patterns including asymmetric loading between the intact and residual limb joints [5] which can cause chronic leg and back pain [6]. The common solution to restore the mobility function is to use prosthetic devices, seen in Figure 1.1 of a lower limb prosthesis user.

1.2 Prosthesis Prior Art

The main goal of lower limb prosthesis design is to restore loss of functionality of the joints, knee, and / or ankle. The ideal prosthetic devices should support and assist the user to complete the daily life tasks without overly exerting their intact joints. Researchers investigated different ambulation conditions in normal life, such as level walking [7], walking on ramps[8], and climbing stairs[9, 10, 11]. In modern days, the most common clinically available prosthetic devices are passive, with few options of powered prostheses available.

1.2.1 Passive Prosthesis

Conventional passive prosthetic devices use only rigid mechanical components to provide support for the user. This type of the prosthetic device does not adapt for the specific activities or tasks the user is completing. It only provides weight-bearing ability when applying load to the prosthetic limb side. Since passive prostheses do not adapt to the user's locomotion patterns, the user may have to increase hip flexion due to restricted knee flexion. At the same time, users have to compensate for hip circumduction with higher vertical displacement of the body [12]. The hip compensation movement introduced asymmetric gait which indicates the bad quality of gait [13]. In recent studies, new mechanisms have been applied and tested in knee and ankle prosthesis design using a spring and damper system [14, 15]. Zelik *et al.* designed a passive ankle-foot prosthesis that applies a spring and damper mechanism to store energy on impact of the foot and release energy in the toe-off phase [14]. Arelekatti and Winter designed a passive knee prosthesis which implemented an automatic early stance lock for stability and differential friction damping system for late stance and swing control [15]. However, these strategies are not efficient as most of the energy is wasted in transmission and difficult to control.

Most commercially available prostheses on the market are passive prosthetic devices. This type of prosthesis can provide variable damping. Microprocessor Prostheic Knees (MPK) are the most common passive prosthesis device in markets and studies [16, 17, 18, 19, 20]. It employs a centered microprocessor with different types of onboard sensors such as encoders, Inertial Measurement Units (IMU) and loadcell. MPKs detect the gait phase of the user and controls the damping of the knee respectively. The typical choices of dampers are hydraulic, pneumatic, or magneto-rheological, which can modulate damping by fluid control [21]. Cao *et al.* proposed an MPK with a hydraulic damper that could continuously adjust knee flexion and extension damping [17]. Lambrecht and Kazerooni designed a hydraulic knee prosthesis by adding power to the device with a pump driven by an electric motor that allows adjustment of the damping during the late swing extension [19]. Park

Figure 1.1: Transfemoral Amputee User on Prosthetic Device

et al. designed a new prosthesis using magneto-rheological damper that can generate a reaction force by controlling the field-dependent yield stress of the magneto-rheological fluid [20]. The benefit of using passive prosthesis is that it can modulate resistances to keep up with the walking speed of the user in level walking. In addition, this type of device is usually lighter in weight and cheaper than an active prosthesis. However, although the passive prosthesis provides resistance during walking, other walking conditions such as ramp ascent and stair ascent remain challenging, as this type of prosthesis cannot produce net positive power to assist users. In addition, the loss of knee and ankle joints increases the load of hip in walking which increases the metabolic cost of the user and fatigue of the hip joint. One solution is to utilize an active/powered prostheses which can yield positive power in knee and ankle joints.

1.2.2 Active Prosthesis

The active robotic prosthesis has been rapidly investigated and studied over the previous decades. An active prosthesis is usually equipped with actuators, sensors, and a microcontroller. Different controller strategies demonstrate different effects on gait outcomes. Several research groups have developed various versions of the knee and/or ankle prosthesis implemented with actuators for generating net positive power with different methods of controllers [8, 22, 23, 24, 25, 26, 27, 28]. These state-of-the-art powered robotic prostheses can recognize the user's locomotion mode using a machine learning method with different approaches such as measuring Electromyography (EMG) signals [23] or data from the sensors onboard [24]. The goal of using an active prosthesis is not only to restore the kinematics of joint movement, but also the kinetics of the joints to assist the user in ambulation when net positive power is needed. Most researchers focus on five different modes of walking: level walking, ramp ascent, ramp descent, stairs ascent, and stairs descent. Sup *et al.* developed a powered knee and ankle transfemoral prosthesis and tested on level walking [29] and sloped walking [8] to replicate the kinematics of knee movement in Able Body (AB) users. Ledoux and Goldfarb investigated the a powered transfemoral prosthesis during walking on a stair ascent using metabolic effort as one of the metrics compared to the passive prosthesis [10].

Although the active prosthesis shows great advantages compared to passive or semi-passive devices, there are only a few powered prostheses clinically available. The gap comes from instability, cost, trust concerns, etc. Any misclassified mode detected by the powered prosthesis during walking may cause the user to fall. This situation will result in the loss of trust of the user to the device. Also, the cost of building a powered prosthesis is significantly higher than other types of devices. Furthermore, the weight of the device is usually heavier than that of any passive device. This drawback might affect comfort when the user is on the device.

1.3 Human Biomechanics

To evaluate the performance of each type of prosthesis, it is not enough to only depend on the control sensor data. One of the most important methods to measure the performance outcomes of these prostheses is to compute the human biomechanics during walking. This analysis should be considered as a holistic view of both the prosthetic side and the intact side. Winter studied the first human lower limb joint biomechanical analysis with hip, knee, and ankle joint kinematics respect to gait cycle [30]. Kaufman *et al.* determined the asymmetry of gait in level walking when using MPK [31]. Ledoux and Goldfarb determined the kinematics and kinetics of active users of transfemoral prostheses on stairs [10]. Nowadays, human biomechanical analysis becomes the key element of examination of the performance outcome.

1.3.1 Whole Body Angular Momentum

Whole Body Angular Momentum (WBAM) is a common metric used to assess balance stability during walking [6, 32, 33, 34, 35, 36, 37, 38]. Pijnappels *et al.* discovered that the regulation of whole body angular momentum can prevent falls and help an individual recover from tripping [39]. The time rate of the change of whole body angular momentum is equal to the net external moment in the body. The net external moment is a function of ground reaction forces (GRFs) and foot placement [36]. During walking, WBAM can be regulated by interchanging the angular momentum of each body segment. Popovic *et al.* described a method to determine the whole body angular momentum($\vec{H}$) about the Center of Mass (COM) as

$$\vec{H} = \sum_{i=1}^{n} [(\vec{r_i}^{\,COM} - \vec{r}_{body}^{\,COM}) \times m_i(\vec{v_i}^{\,COM} - \vec{v}_{body}^{\,COM}) + I_i\vec{\omega_i}] \tag{1.1}$$

where $\vec{r_i}^{\,COM}$, $\vec{v_i}^{\,COM}$, and $\vec{\omega_i}$ represent the position, linear velocity, and angular velocity of the body segment in the COM of each segment of the segment. $\vec{r}_{body}^{\,COM}$ and $\vec{v}_{body}^{\,COM}$ represent

the position and linear velocity of the whole body COM. m_i and I_i represent as the mass and moment of inertia properties of each body segment. Finally, *n* represents the number of body segments to compute the whole body angular momentum.

In previous studies, Popovic *et al.* introduced the angular momentum control in level walking [36]. Silverman *et al.* completed studies of AB whole body angular momentum on incline and decline walking [34], on stair ascent and descent walking [35], and turning 90-degree turns [33]. There are also studies on the whole body angular momentum evaluation of lower limb amputees. Silverman and Neptune tested the effect of different walking speeds on WBAM for individuals with below-knee amuptation [37]. D'Andrea *et al.* evaluated the assistance of passive and powered ankle prosthesis in the regulation of WBAM during walking at different speeds [38]. It is now known that the prosthesis can help individuals with below-knee amuptation better regulate whole body angular momentum during walking, especially with a powered ankle prosthesis device [32].

1.3.2 Able Body Biomechanics

In recent decades, as motion capture technology has developed, the researchers worked on human locomotion in different walking conditions and environments. Ankaralı *et al.* studied the gait symmetry in dynamic walking in different walking speeds [40]. Riener *et al.* investigated the Inverse Kinematics (IK) and Inverse Dynamics (ID) of walking in different stair heights [9]. Furthermore, Camargo *et al.* published an opensource data of lower limb biomechanics in stairs, ramps and level walking [41]. This study demonstrated that the human joints can modulate both kinematics and kinetics at different conditions of each ambulation mode.

1.4 Motivation

Although several studies have shown that powered ankle-foot prostheses can help individuals with below-knee amuptation regulate the angular momentum of the entire body for

better balance stability control, there is still a gap in the evaluation of individuals with transfemoral amuptation balance stability. This thesis study will focus on three different commercially available MPKs in two different types of knee prosthesis devices, which are passive and active, in a Narrowing Beam Walking Test (NBWT) and evaluate the performance of each knee in stability control for transfemoral amputees, discussed in Chapter 2. The goal of this chapter is to characterize each MPK and define the differences in functional performances. I hypothesize that using active MPK can outperform on the regulation of whole body angular momentum than passive MPK during narrowing beam walking test. Another goal of this study is to define the WBAM threshold during beam walking when amputees fall.

By the inspiration of able body biomechanics, rehabilitation of knee and ankle joints aided by the powered prosthesis would be tremendously beneficial for the transfemoral amputees. Some powered prostheses in the research phase can modulate the user's walking speed, but there is still a gap in yielding scaling assistance in stairs and slope walking. This thesis study will focus on the scaling assistance in ramp walking at different inclination angles for transfemoral amputees using powered knee ankle prostheses, discussed in Chapter 3, 4 and 5. The goal of these chapters is to build a controller that generates a biologically inspired modulation of knee kinematics, kinetics, and joint power.

CHAPTER 2

NARROWING BEAM WALKING TEST BALANCE STUDY

2.1 Overview

This chapter analyze the effect of three different commercially available microprocessor knees in the market on balance stability control of the lower limb prosthesis users. The following sections include the methodology, results, and discussion of these users on the narrowing beam walking test, mainly using WBAM as outcome metrics.

2.2 Methodology

2.2.1 Experimental Devices

Narrowing Beam Walking Test

Due to the loss of the lower limb, falls are one of the most frequent and common risks that lower limb prosthesis users experience in the daily life. The consequences of falls can result in both physical and psychological effects, including injuries, limitations in activities, and reduced quality of life [42]. Thus, balance stability improvement has been one of the leading targets in designing lower limb prostheses. Contemporary clinical balance tests, such as Berg Balance Scale (BBS), Activities-specific Balance Confidence (ABC), Four Square Step Test (FSST), etc., cannot generate sufficient information on the ability to control stability. BBS cannot discriminate between individuals with a higher or lower risk of falling [43]. ABC scale test cannot discern the differences between users of transtibial and transfemoral lower limb prostheses [44]. FSST has not been validated among new lower limb prosthesis users [45]. Any clinical balance tested that is too easy or too hard for people with moderate impairments will show floor or ceiling effects. Thus, there is a need for a more suitable clinical balance test designed for lower limb prosthesis users.

Sawers and Hafner designed a Narrowing Beam Walking Test (NBWT) that can differentiate the level of stability control of balance among users of lower extremity prostheses [46, 42] shown in Figure 2.1. The narrowing beam consists of four different fixed-width segments at 18.6 cm, 8.6 cm, 4.0 cm, and 2.0 cm. Each segment of the beam is 1.83 m long and the total beam length is 7.32 m. NBWT challenges balance control by constraining step width and support surface. Participants are asked to cross arms over the trunk and walk along the narrowing beam. The distance traveled along the beam is defined as when the participant steps off the beam, uncrosses arms, or finishes the entire length of the beam and is used as outcome metrics. Sawers and Hafner validated the NBWT can discriminate the performance of different users of lower extremity prosthesis without floor or ceiling effects [42].

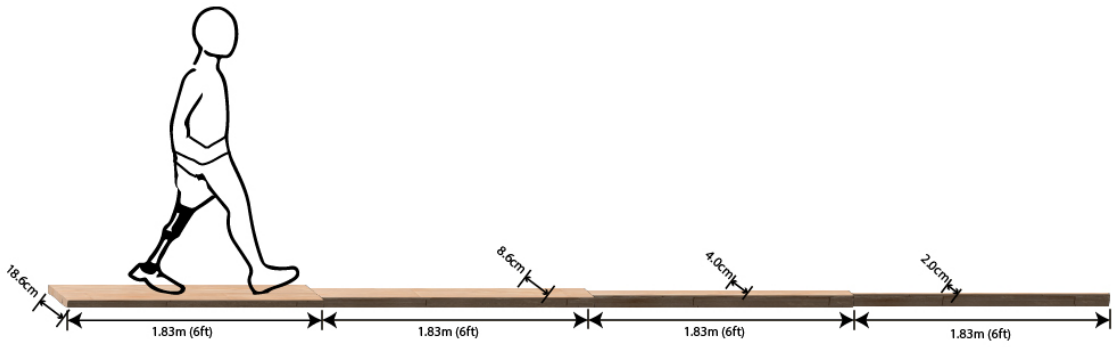

Figure 2.1: Lower Limb Prosthesis Users on NBWT.

Microprocessor Knees

This study uses three different commercially available MPKs, which are Cleg 4.0 (Ottobock), RheoKnee (Össur) and PowerKnee (Össur). Cleg 4.0 and RheoKnee are passive knee prosthetic devices, while PowerKnee is an active / powered knee prosthetic device. One previous study indicated that both Cleg 4.0 and RheoKnee can yield adaption of resistances to different movements but Cleg 4.0 showed better natural knee function when compared to the contralateral side [18]. Another study discovered that the C leg demonstrated a more reliable side load bearing capacity than RheoKnee [47]. Highsmith *et al.*

described the kinetic profile of transfemoral individuals in the sit-to-stand motion, which the Power Knee provides a better symmetry in knee moment when sitting down compared to standing up [48]. Albeit these studies ran the comparisons between three different MPKs, they only considered normal movements and have not evaluated any stability performances. Therefore, this study compares the stability control of three different MPKs in transfemoral individuals in the NBWT.

2.2.2 Experiment Protocol

Individuals with unilateral transfemoral amputation (N=2 subjects, encoded as MPK01 and MPK02, two males, age: 51 $\pm$ 15.5 years, mass: 89 $\pm$ 13 kg, height: 1.86 $\pm$ 8.5 cm) provided with informed consent forms for this study which was approved by the Georgia Institute of Technology Institutional Review Board (IRB). Subjects were asked to participate in four visits throughout the study. In the first three visits, the subjects were fitted and aligned with the prosthetic knees in random order with a training and tuning process. Subjects would bring the prosthetic device home for one week when they felt comfortable walking over various terrains in the lab space, including overground, stairs, and ramps. The take-home process was completed to acclimate to the device to avoid bias in data collection. Participants also used their original socket, prosthetic foot, and shoe during each knee evaluation to ensure that the differences observed during the study are attributable only to the knee. From the second to the last visit, the subjects ambulated on ramps, stairs, a gait mat, and a narrow beam, while this study only focuses on the beam walking section. In data collection sessions, subjects were asked to perform NBWT for five trials in each knee, of which 3 to 5 trials will show steady performance [42]. The experiment used 3-D motion capture system (Vicon, Oxford, UK) to record the kinematics of the subject. A static pose was recorded before conducting NBWT for model scaling purpose. During beam walking, subjects were recorded with motion capture data with arm crossed after marking up with full-body marker set shown in Figure 2.2. The same process was completed on all three

MPKs.

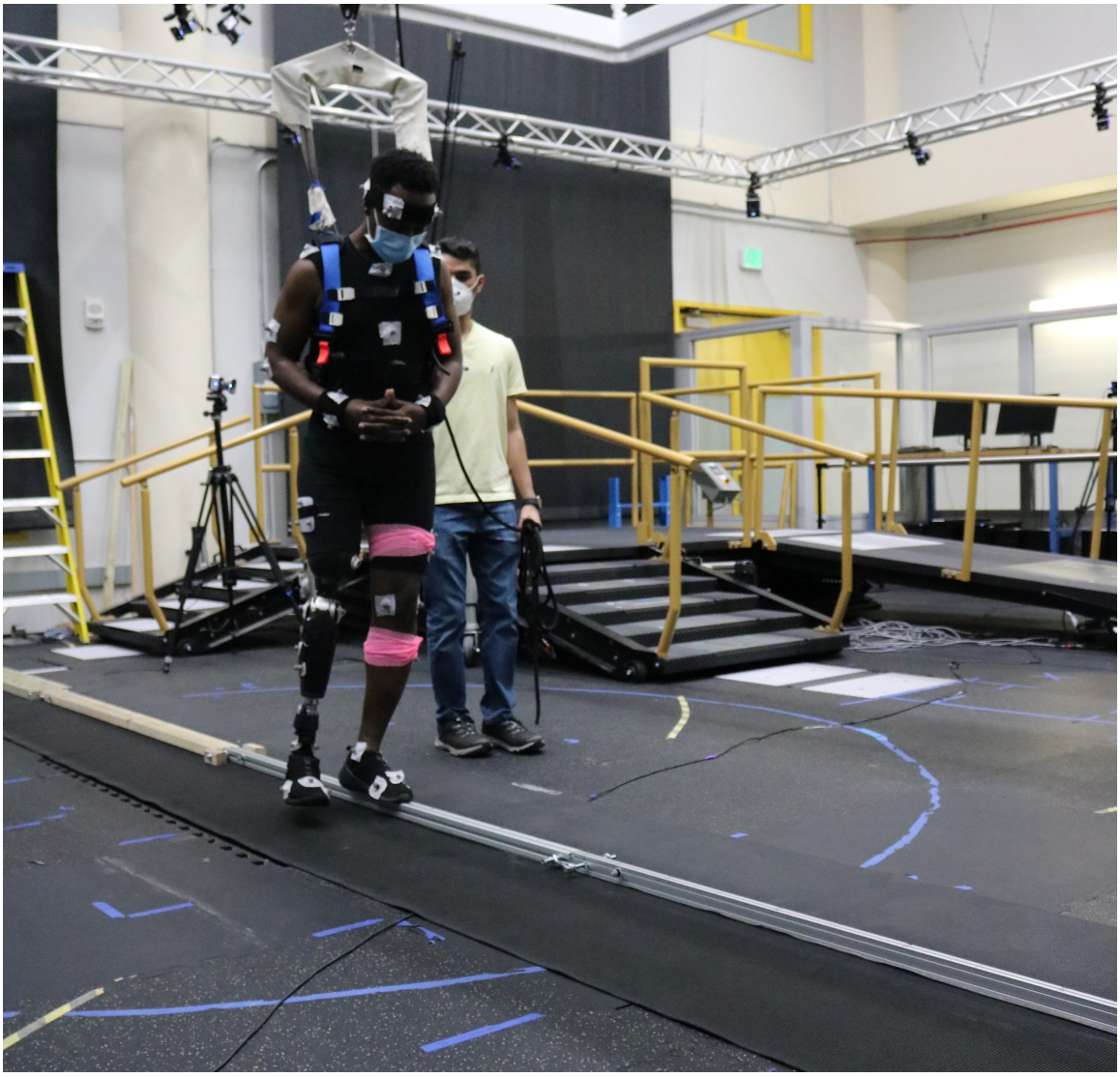

Figure 2.2: Narrowing Beam Walking Test During Experiment

2.2.3 Biomechanics

To extract the biomechanical information of the subject from the motion capture system, OpenSim, an opensource simulation software [49], is used with a customized musculoskeletal model shown in Figure 2.3 as an example of unilateral lefty transfemoral amputee. The model consists of all human body segments except the prosthetic knee side. The prosthetic side is impaired with a model of Cleg 4.0 connecting the prosthetic knee

joint to the residual femur and a model of ProFlex Foot (Össur). The marker set of the model includes 51 markers in total. The four markers on the pelvis, four markers on both knees, and four markers on both ankles are distributed with the highest weight in the set-up to focus on the control of the lower extremities. Markers on the torso, head, two arms, and wrists are used to determine the angular momentum of the upper extremities. Markers on the thigh and shank are used to fill rigid body gaps in motion capture data processing.

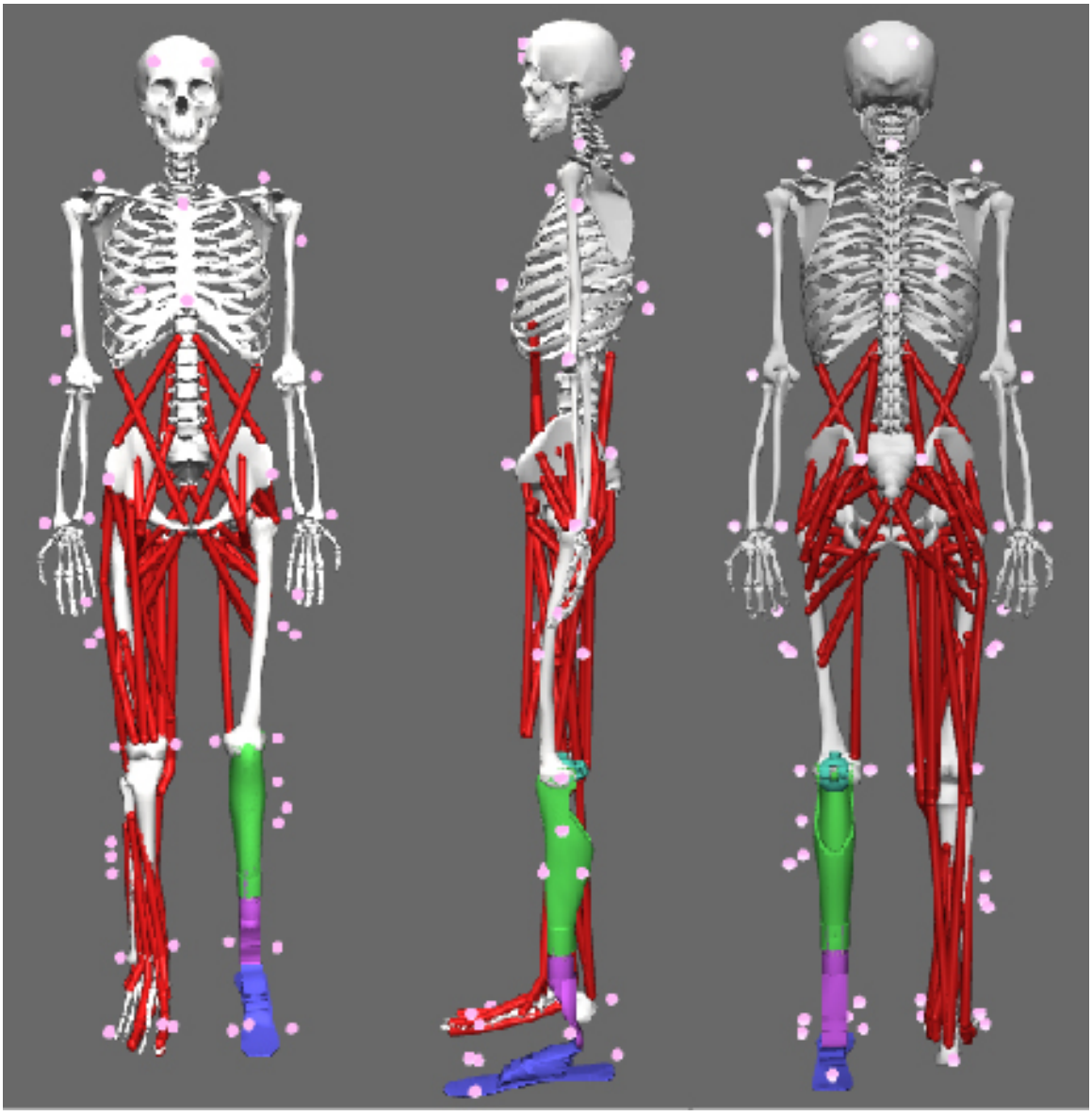

Figure 2.3: OpenSim Musculoskeletal Model with Prosthesis

There are two workflows in biomechanical data generation: (1) Scale and (2) Inverse

Kinematics. The scaling process includes the adjustment of the size of each of the biological segments and the length of the pylon of the prosthesis. It will extract the labeled markers from the previous recorded static pose trial and determine the scaling factors of each bone segment based on the relative distances between the markers. For example, to scale the prosthesis pylon, the length of the pylon is calculated based on the distance between two markers, which are the left lateral knee (LLKNE) and the left lateral ankle (LLANK). The marker positions in the model are adjusted to match the static motion capture data by least squares fitting. In the inverse kinematics work flow, it extracts the processed motion capture data from subjects walking on the beam and uses the scaled model as the baseline to run the inverse kinematics tool. When running the inverse kinematics process, each marker is associated with different levels of weight and is selected with increased weight relative to other markers. The weight difference is typically ten times that of the norm.

Whole body angular momentum, distance traveled and stride metrics are used as the outcome metrics in this study. Body segment position data with time series can be determined from the inverse kinematics results from OpenSim. The linear velocity and the angular velocity can be computed by dividing the position result. Thus, the body segment angular momentum and whole body angular momentum can be determined using Equation 1.1. The distance traveled is marked by the event of falling or uncrossing arms. These two events can be determined from the vertical coordinates of the foot markers and the velocity of the wrist markers. The distance from the most anterior position of the last foot on the beam was recorded as the distance traveled. Stride metrics includes the stride time, symmetry index and foot placement. The events of heel contact and toe off are found using the foot markers since there is no force data to detect. Thus, the stance time, swing time, and stride time can be computed using this strategy.

2.3 Results

2.3.1 Distance Traveled and Stride Time on NBWT

Figure 2.4 indicates the distance traveled of each subject using three different MPKs on NBWT. Although PowerKnee and RheoKnee each traveled the furthest on the beam in two different users while Cleg 4.0 performs the worst, RheoKnee indicates a more stable performance in both subjects than PowerKnee. In Figure 2.5, both subjects demonstrated a symmetric gait during beam walking. It is also important to note that MPK02 spends more time on each step which results in a longer distance traveled compared to MPK01.

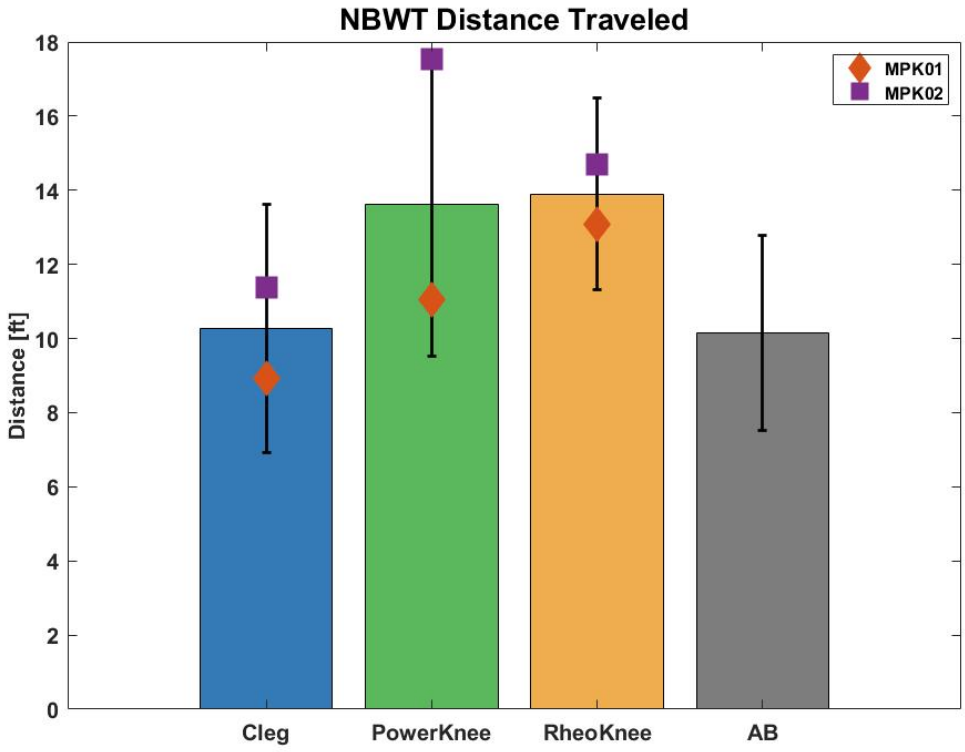

Figure 2.4: Distance Traveled on NBWT

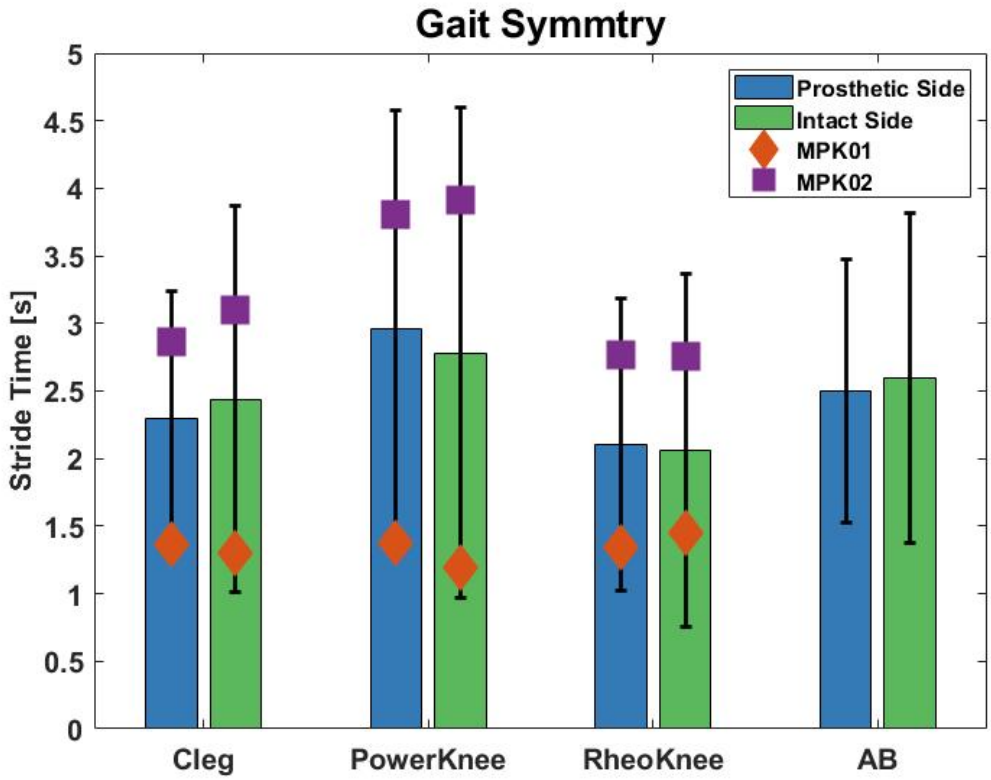

Figure 2.5: Stride Time on NBWT

2.3.2 WBAM Comparison Between AB and TF on NBWT

Below in Figure 2.6 and Figure 2.7 is the overview of WBAM during beam walking for an AB subject and two subjects in the three MPKs (Cleg 4.0, RheoKnee and PowerKnee) in the sagittal, frontal and transverse planes. These WBAM curves were averaged in all segments of the five trials. The WBAM values were also semi-normalized by the height and mass only. WBAM cannot be normalized by the walking speed, as it varies drastically during beam walking. This plot represents the general performances as individual in beam walking in respect to the gait cycle. Generally in the sagittal plane, there are no significant differences between AB subjects and transfemoral individuals in averaged WBAM, except MPK02 (red curves) showed a worse regulation of WBAM using RheoKnee. Surprisingly, MPK01 had a better sagittal plane WBAM regulation compared to AB subject. In frontal plane, MPK01 (blue curves) showed relatively higher deviation values with all micropro-

cessor knees than AB subject. In the transverse plane, there is no significant difference between the AB subject and the individuals with TFA.

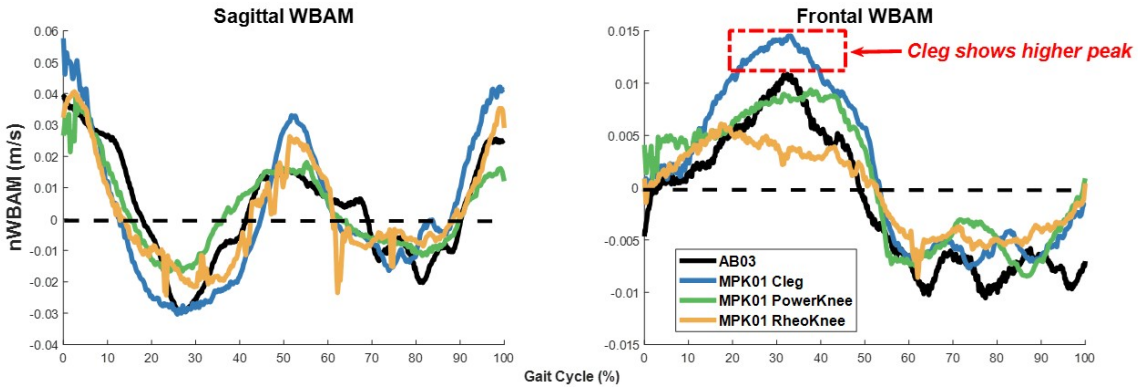

Figure 2.6: Whole Body Angular Momentum Comparison between AB Subject and Unilateral Transfemoral Subject MPK01 on the Narrowing Beam Walking Test

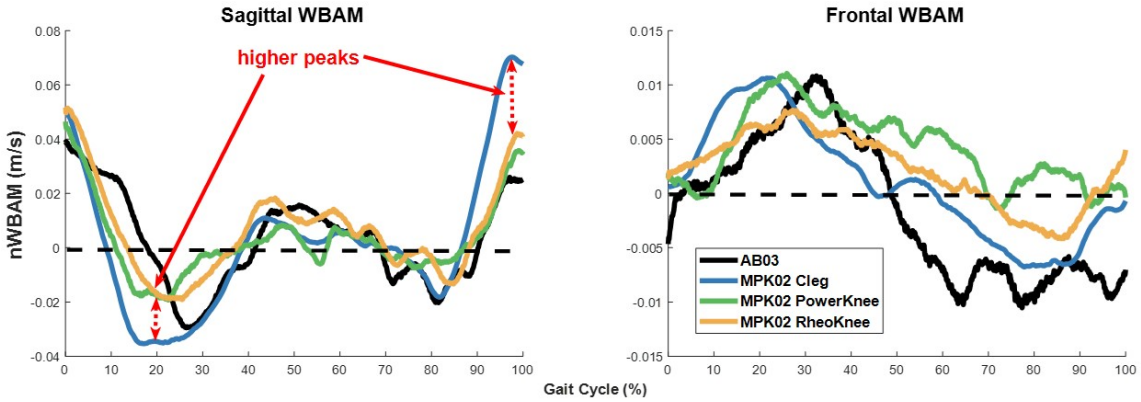

Figure 2.7: Whole Body Angular Momentum Comparison between AB Subject and Unilateral Transfemoral Subject MPK02 on the Narrowing Beam Walking Test

2.3.3 IK and WBAM among All MPKs on NBWT

Inverse kinematics of subject MPK01 and WBAM comparison of each subject, MPK01 and MPK02, across all three MPKs are shown in Figure 2.8 and Figure 2.9. Both results were segmented with respect to the gait cycle across all beam segments without normalization.The comparisons are evaluated only among MPKs. Both Cleg 4.0 and RheoKnee showed similar kinematics across all three joints either in prosthetic or intact side. PowerKnee exhibited a higher knee swing flexion angle compared to the other two devices. In

the WBAM comparison, all three MPKs showed almost identical results in sagittal plane for MPK01 while showing the opposite results for MPK02. In both frontal and transverse plane, RheoKnee exhibited higher averaged WBAM ranges. Furthermore, although the average Cleg 4.0 WBAM values were correlated with PowerKnee, Cleg 4.0 showed the largest variation in these two planes.

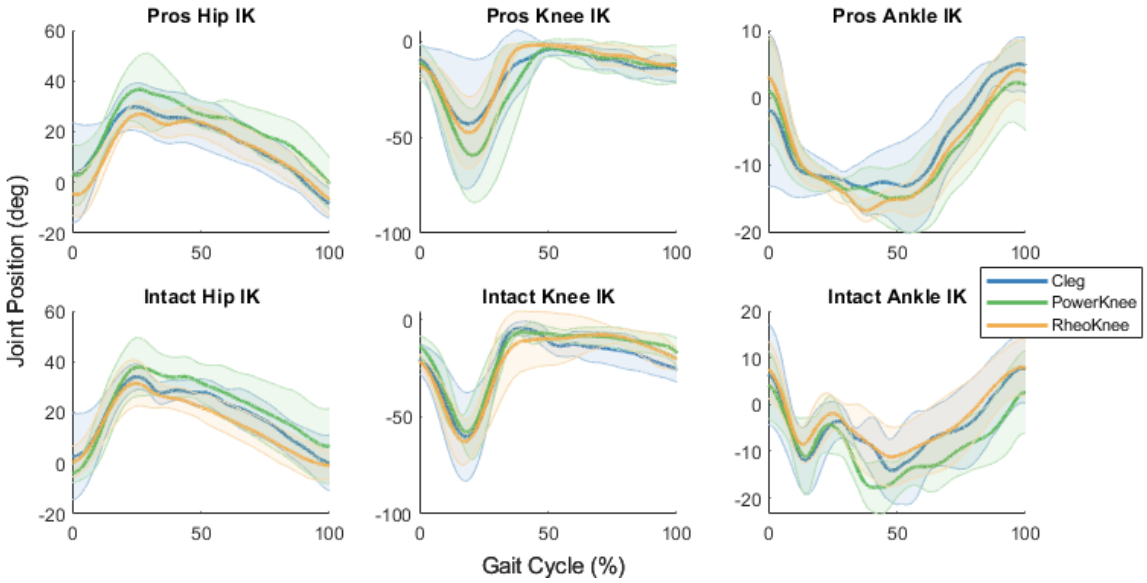

Figure 2.8: Inverse kinematics result segmented in gait cycles across all three microprocessor knees

2.3.4 WBAM at the Last Gait Cycle on NBWT

Figure 2.10 shows a the comparison between the last gait cycle with other gait cycles. The last gait cycle is defined in the event of a fall detected by foot markers. Other gait cycles are represented as the averaged WBAM of all previous steps before the fall within the same trial among all MPKs. During the last gait cycle, both mean and standard deviation of the WBAM during the stance phase are higher than other gait cycles in the sagittal plane. In the frontal plane, WBAM of the last gait cycle can be easily discriminated from WBAM of other gait cycles such that the WBAM of the last gait cycle shows a significant larger deviation.

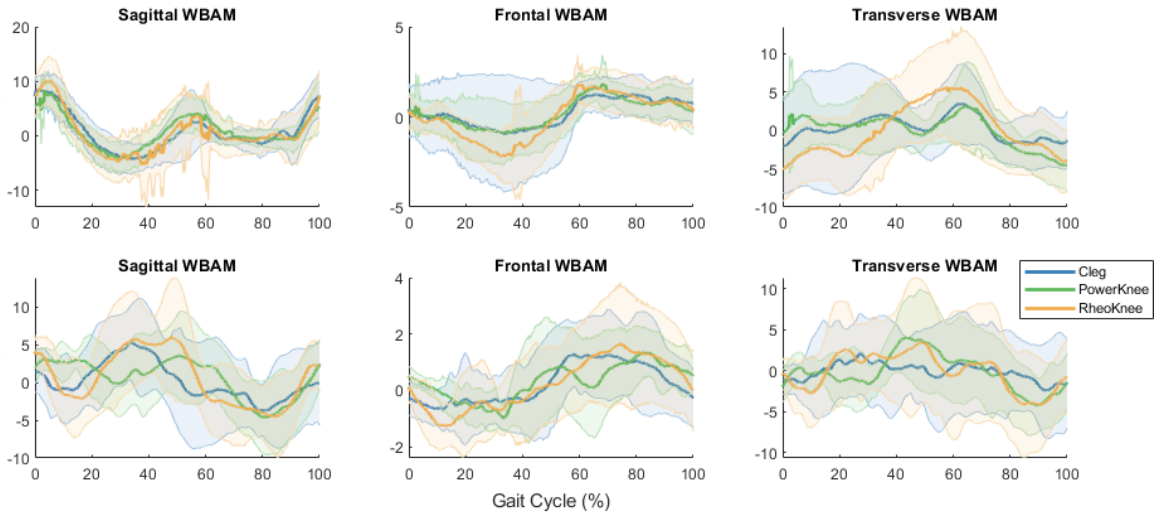

Figure 2.9: Whole body angular momentum result segmented in gait cycles across all three microprocessor knees

2.3.5 WBAM at Each Segment of the Beam on NBWT

Figure 2.11 and Figure 2.12 separately demonstrated the WBAM evaluation of MPK01 and MPK02 in each beam segment. Seg1 to 4 represent segments 1 to 4 of the beam. Seg12 to 34 represent the transition phase of the beam from one to another. In the sagittal plane, both MPK01 and MPK02 showed that variation gradually increases as they walked further on the beam. The magnitude of the averaged WBAM at each segment in the sagittal plane did not change much. However, both MPK01 and MPK02 tend to spend more time in the early stance phase as they walk further. Such a phenomenon is also exhibited for MPK02 in the frontal plane. WBAM for MPK01 in frontal and tranverse plane did not imply any patterns for each segment.

2.3.6 Peak-to-Peak WBAM on NBWT

WBAM regulations are quantified using the peak to peak value shown in Figure 2.13. Despite some initial segments trial with bad marker quality are ignored, it clear that the peak-to-peak WBAM values gradually increases as the beam gets narrower although the event of fall might occur at any segments. In MPK01, PowerKnee exerts better regulation in sagittal

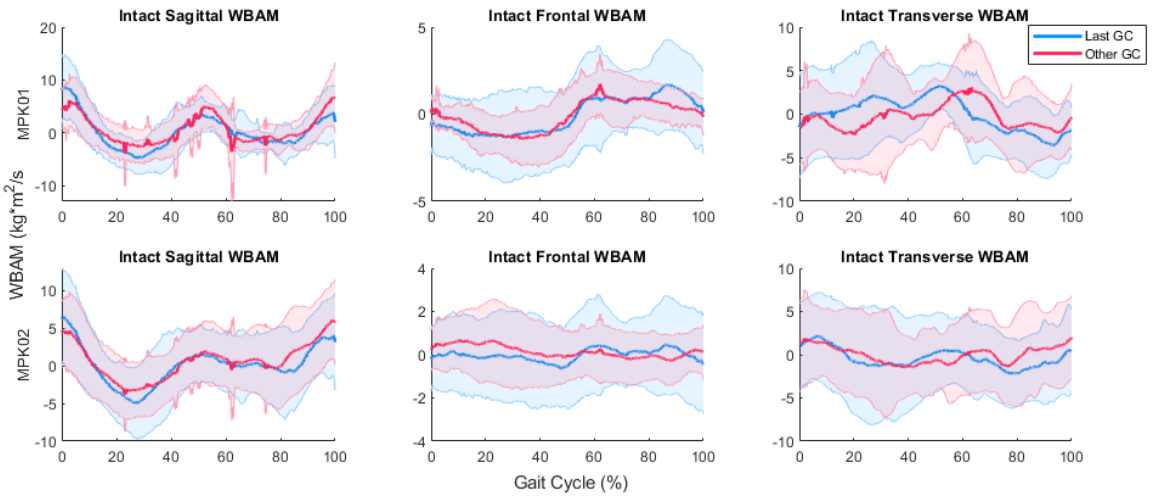

Figure 2.10: WBAM evaluation at the last gait cycle of the beam

and transverse plane than RheoKnee in narrower segments, but RheoKnee performs better in frontal plane. In the 2 subjects tested, Cleg 4.0 performed the worst and did not go beyond transitions from second segment to the third segment of the beam. In MPK02, all three MPKs demonstrated a similar result until the third segment of the beam in the sagittal plane. PowerKnee shows a better control of WBAM at the further segments compared with RheoKnee. In the frontal plane, RheoKnee indicated a more stable control of WBAM than PowerKnee. In the transverse plane, PowerKnee operated better than RheoKnee in further segments with smaller peak-to-peak WBAM and deviation values.

2.4 Discussion

This study is designed to evaluate the stability control of lower limb prosthesis users with different MPKs and discern the WBAM holistically at the event of falling. Across two subjects, Cleg 4.0 showed the worst performances in several aspects despite the feedback from both subjects indicating Cleg 4.0 as their most favorable device among all three. Surprisingly, PowerKnee shows relatively good performances in distance traveled and WBAM after both subjects expressed frustration on PowerKnee. RheoKnee demonstrated steadily good results, but with unstable WBAM regulations. All three MPKs can restore gait sym-

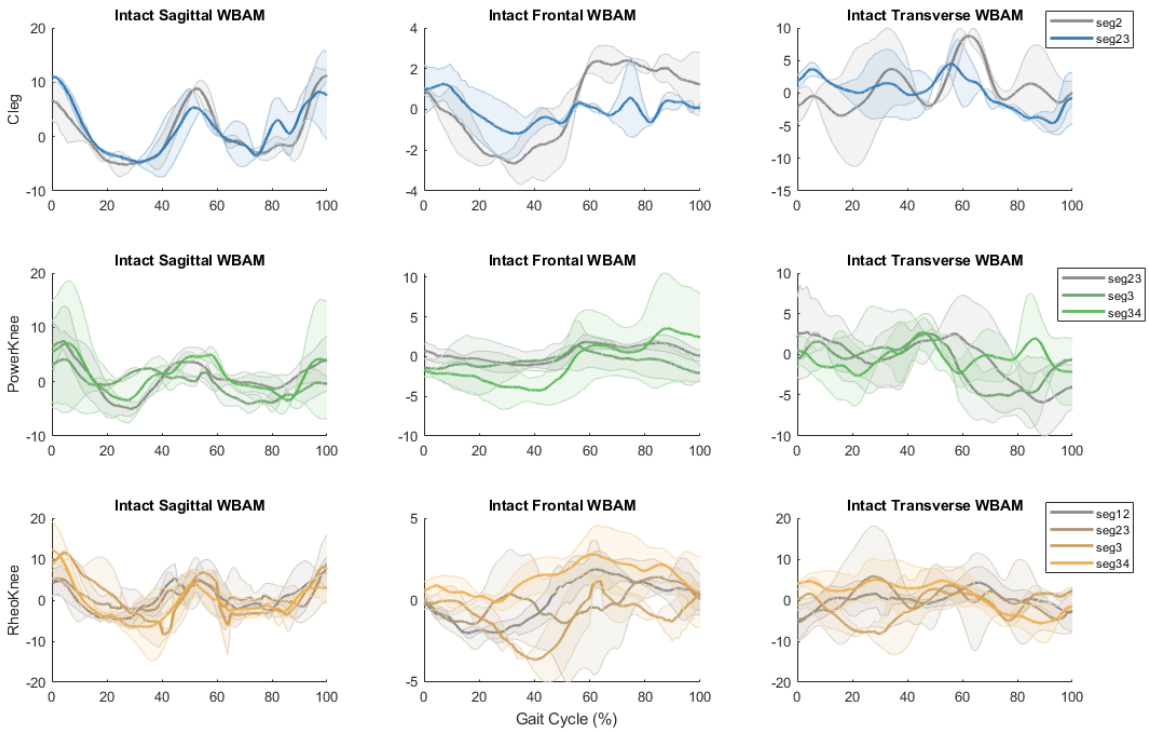

Figure 2.11: MPK01 WBAM evaluation at each segment of the beam

metry as the stride time on each limb are comparatively equal with almost identical kinematics provided by MPKs.

Cleg 4.0 has the feature of intuitive stance which automatically activates to fully block the knee from bending after maintaining at the same pose for two seconds. RheoKnee has the feature to scale the resistances based on the loading on the prosthetic knee. RheoKnee can yield more resistances with more loading until there is no bending. PowerKnee has a similar feature as Cleg 4.0 with intuitive knee lock function which the microprocessor can detect if the user is in stand and lock the knee at that moment. This correlates to the performance of the beam walking distance which indicates their stability control. Although the three MPKs facilitate the knee support features by locking or yielding resistances, the methods for activating such features are different. Cleg 4.0 requiring the user to spare a few seconds in the same knee flexion might be too long. The stride time of MPK01 on the prosthetic side is less than two seconds, which might not trigger the intuitive stance feature properly. The stride time of MPK02 on the prosthetic side is significantly longer

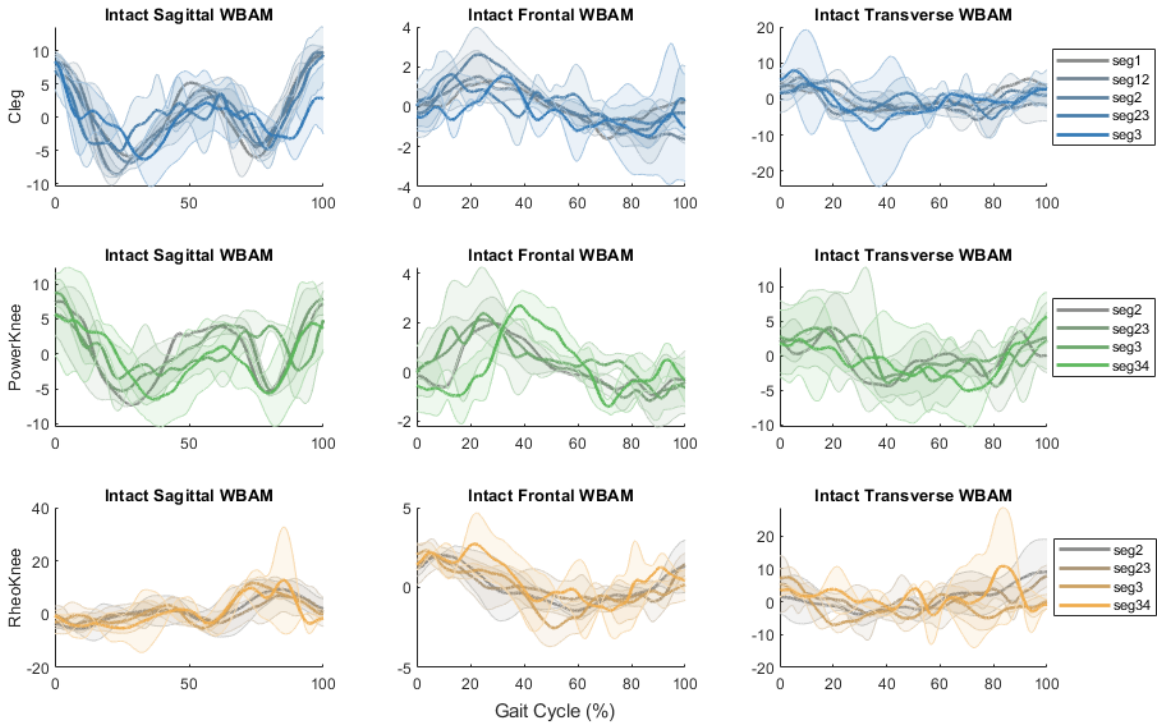

Figure 2.12: MPK02 WBAM evaluation at each segment of the beam

than MPK01 and reach up to almost four seconds. Such a large difference can differentiate the stability control ability of the device as MPK02 notably performed better than MPK01. PowerKnee knee stance lock is triggered by the detection of the sensors. The detection might not be accurate if the user is doing any non cyclic tasks like beam walking. This can result in very different balance outcome across different users as shown in Figure 2.4. RheoKnee can produce resistance, regardless of the current ambulation mode or the time spent in the knee stance phase, with more load. This results in the steady distance traveled on the beam walking. Also, the result shows that most falls occur when the prosthetic foot cannot make proper contact with the beam and lose stability at that moment. The detour of the prosthetic foot of the subject before landing on the beam is when the subject uses their hip joints to compensate for balance while swinging the contralateral limb.

When compared to WBAM at different conditions, Cleg 4.0 shows the largest deviation especially in the frontal plane within the same user. The upper limb angular momentum is constrained by asking the subject walking on the beam while crossing the arms. The

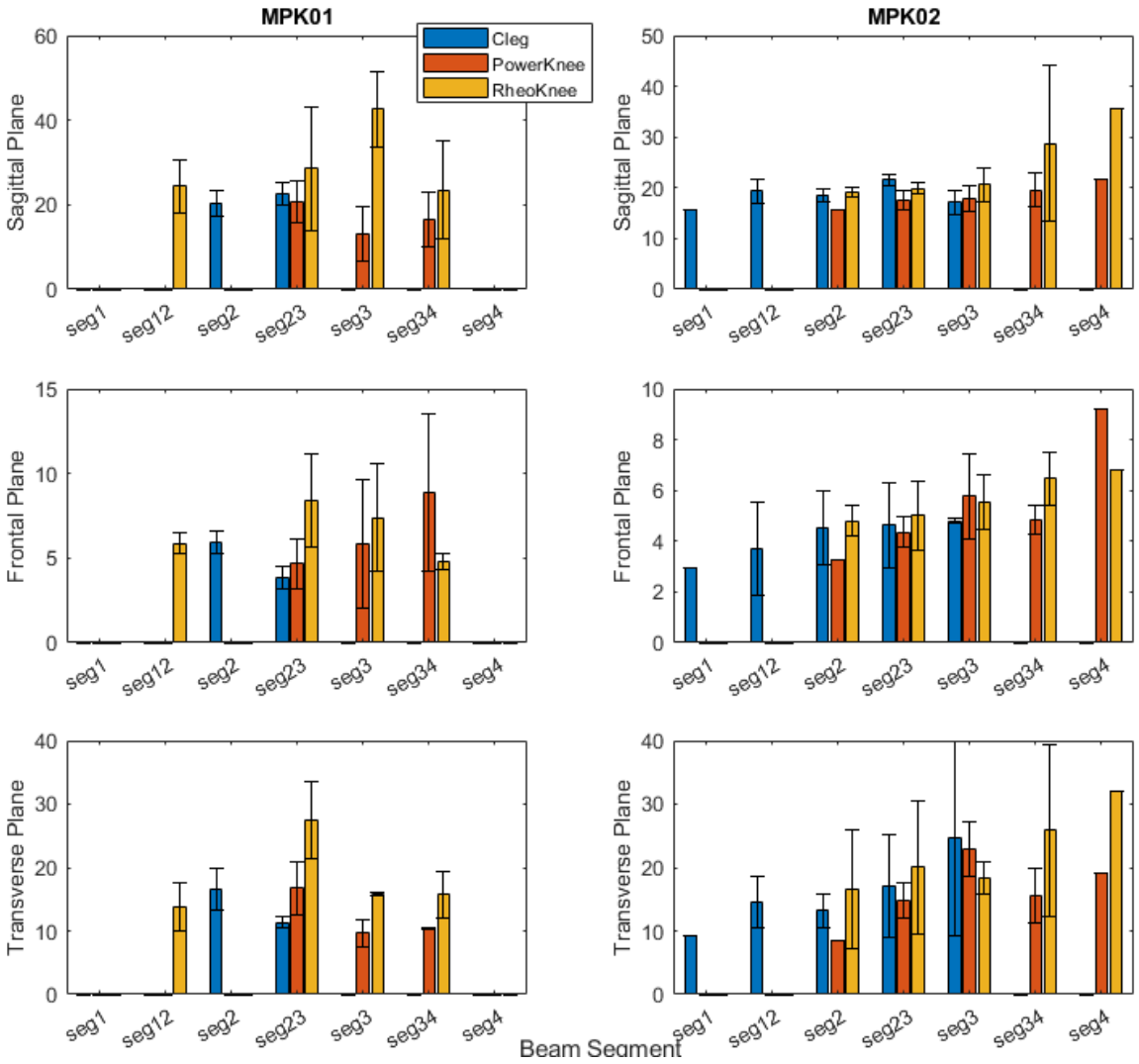

Figure 2.13: WBAM Peak to Peak

dominant body segment attribution to whole body angular momentum will be the movement of the hip and ankle, where MPK has no control of the hip and ankle joints. However, the weight of the MPK device can affect the regulation of the WBAM during the prosthetic swing phase. Cleg 4.0, PowerKnee, and RheoKnee weigh 1.24kg, 2.7kg, and 1.6kg each. The similar weights of the prosthesis compared with their intact limb weights can compensate for the COM position, which ultimately affects WBAM during beam walking.

Both MPK01 and MPK02 showed increases in the WBAM range in both the sagittal and frontal planes. The sagittal WBAM did not show much change except for small increases in

deviation in the narrower segments, while the frontal WBAM exhibits the greatest change in the narrower segments. Compared to the WBAM of the last gait cycle with that of other gait cycles, the frontal WBAM shows a significant increase in the range of WBAM, which is also demonstrated in peak-to-peak WBAM values. This change might be correlated with foot placement during beam walking. The most common causes of falling during the NBWT by observation and motion capture data review is the incorrect prosthetic foot placement. As the beam segments get narrower, the contact surface area reduces more, which can cause the lower extremity amputee to miss the foot placement. Loss of foot proprioception has a tremendous impact on their balance control. In **??**, when the subject did not contact his prosthetic foot, the COM will accelerate vertically, resulting in a higher peak value in the frontal WBAM measurement. It is clear that there is a threshold in frontal WBAM to detect the falling event, but the actual value might not be feasible to determine with only two subjects data.

CHAPTER 3
INITIAL OSL BIOMECHANICS STUDY

3.1 Overview

This chapter explains the first iteration of Open-Source Leg biomechanics testing with a biologically inspired slope walking controller. The following sections include methodology, result, and discussion of the biomechanical outcomes of unilateral transfemoral amputees walking on ramps using active prosthesis and passive prosthesis.

3.2 Methodology

3.2.1 Experimental Device

Most of the active/powered prosthetic devices are still in research phase. One of these devices is the Open-Source Leg (OSL) designed the University of Michigan which is a knee and ankle prosthesis with two Series Elastic Actuators (SEA) shown in Figure 3.1. This two Degree-of-Freedom (DOF) prosthesis can provide the knee-and-ankle positive power and movements in the sagittal plane only. Besides two motors, the device consists of two types of encoders in two joints: motor encoders and joint encoders, one 6-DOF loadcell to measure the forces and moments in three directions mounted externally between the adjustable pylon configuration, one 6-DOF shank IMU to measure acceleration and gyroscopic information. All sensors are collaborated with the microcontroller, Raspberry Pi. The specs of the device are shown in Table 3.1. The Range of Motion (ROM) of knee ranges from 0° to 120° knee flexion while ROM of ankle ranges from 20° dorsiflexion to 10° plantarflexion. The purpose of using the OSL is to unify multiple research collaborations for comparison of control systems on the same knee-and-ankle prosthetic device.

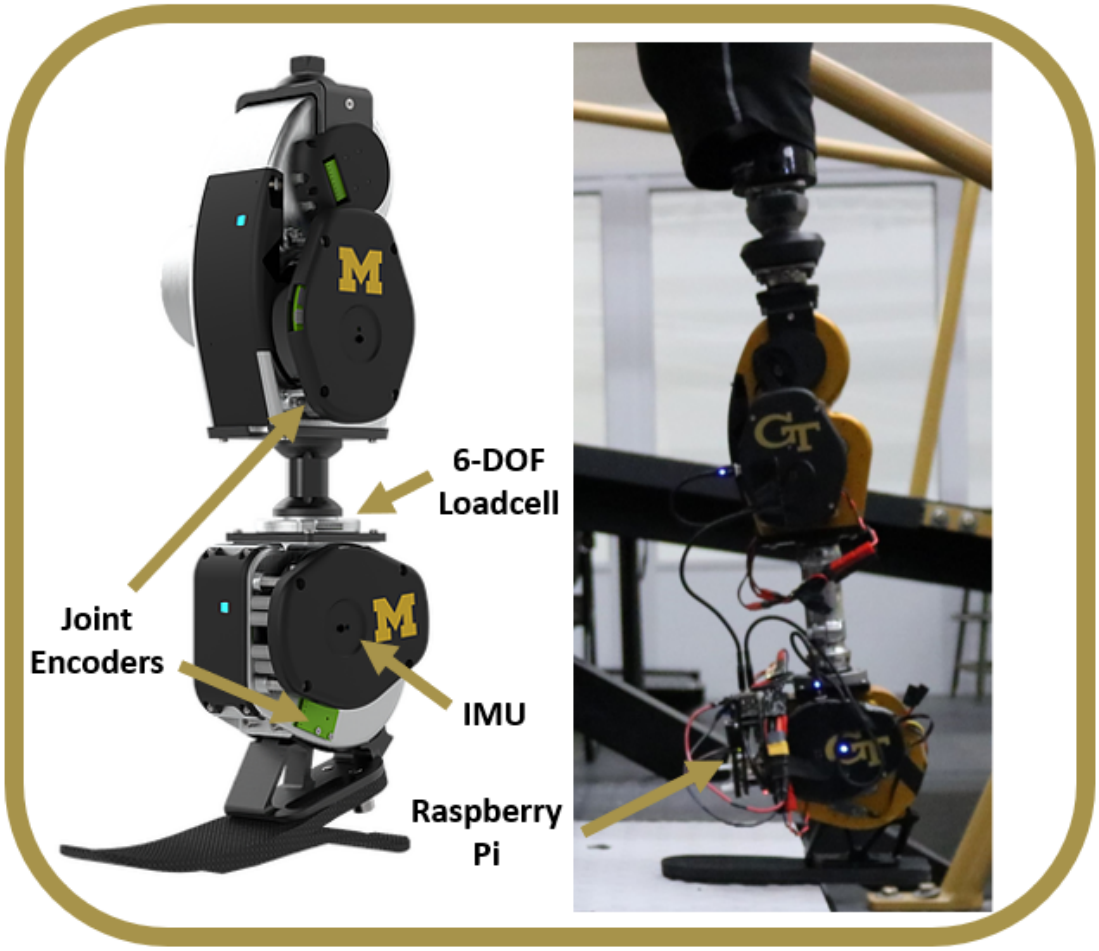

Figure 3.1: Open-Source Leg

3.2.2 Control Paradigm

OSL is implemented with a hierarchical control paradigm [27] including a high-level, mid-level and low-level controller.

The high-level controller is focused on determining which locomotion mode a user is in using machine learning and intent recognition systems. This allows the user to ambulate in different modes such as level walking, stair ascent/descent, and ramp ascent/descent, etc. This controller typically utilized the sensor data from OSL as the training data and ran through a machine learning algorithm to generate models for mode classification and regression to aid users to adapt to different modes automatically.

The mid-level controller is focused on determining the desired torque for both knee

Table 3.1: Open-Source Leg Specs

Parameter	Knee	Ankle
Mass (g)	2160-2330	1740
Height (mm)	240	213
Range of Motion (°)	120	30
Torque Constant (Nm/A)	0.096	0.096
Peak Torque (20 sec) (Nm)	125	148±41
Peak Speed (rad/s)	5.2	5.6

and ankle joints at different modes and phases. The mid-level controller is implemented using impedance controller shown in Equation 3.1 in conjunction with the Finite State Machine (FSM). τ represents the desired or commanded torque. k and b each represents as the stiffness and damping coefficient of the controller using series elastic actuators. θ, θ_{eq} and $\dot{\theta}$ each represents the current angle, desired angle, and angular velocity. The finite state machine was segmented to four phases and four transitions for each mode. There are two stance phases: Early Stance and Late Stance, and two swing phases: Swing Flexion and Swing Extension. Impedance parameters can be changed for each phase in all modes. Transitions between phases are determined using the sensor data. T1 represents the transition between Early Stance to Late Stance using ankle angle threshold. T2 represents the transition between Late Stance to Swing Flexion using the load (vertical force) data threshold. T3 is the transition between Swing Flexion to Swing Extension using knee angular velocity threshold. T4 is the transition between Swing Extension to Early Stance using the load (vertical force) data threshold. All transitions are added with a minimum time threshold to prevent transitions triggering too soon.

$$\tau = -k(\theta - \theta_{eq}) - b\dot{\theta} \tag{3.1}$$

The low-level controller is a basic PID controller to ensure the applied torque tracks with the desired torque using the feedback closed loop control.

The focus of this study is on the mid-level controller to generate a biological inspired scaling controller for unilateral transfemoral prosthesis users. In addition to the fundamental mid-level controller, Simon *et al.* proposed five more control strategies to provide comfortable ambulation across a range of transfemoral amputees [50] (p represents as impedance paramters in the follwing equations if not specified):

1. Constant Impedance Based on Previous State:

$$p_{threshold} = previous \tag{3.2}$$

2. Scale On Ankle Stiffness Equation where W was body weight:

$$k_{ankle} = W(0.237\theta_{ankle} + 0.028) \tag{3.3}$$

3. Damping Equation where P was a constant less than 1:

$$\theta_{knee} = P(\theta_{knee}) \tag{3.4}$$

4. Scale on Weight Equation of decreasing load where C was scaling factor, F was load:

$$p_i = C_i(\frac{F - F_{Initial}}{F_{Initial} - F_{Final}})(p_{i,Initial} - p_{i,Final}) + p_{i,Initial} \tag{3.5}$$

5. Scale on Weight Equation of increasing load where C was scaling factor, F was load:

$$p_i = C_i(\frac{F - F_{Final}}{F_{Final} - F_{Initial}})(p_{i,Initial} - p_{i,Final}) + p_{i,Initial} \tag{3.6}$$

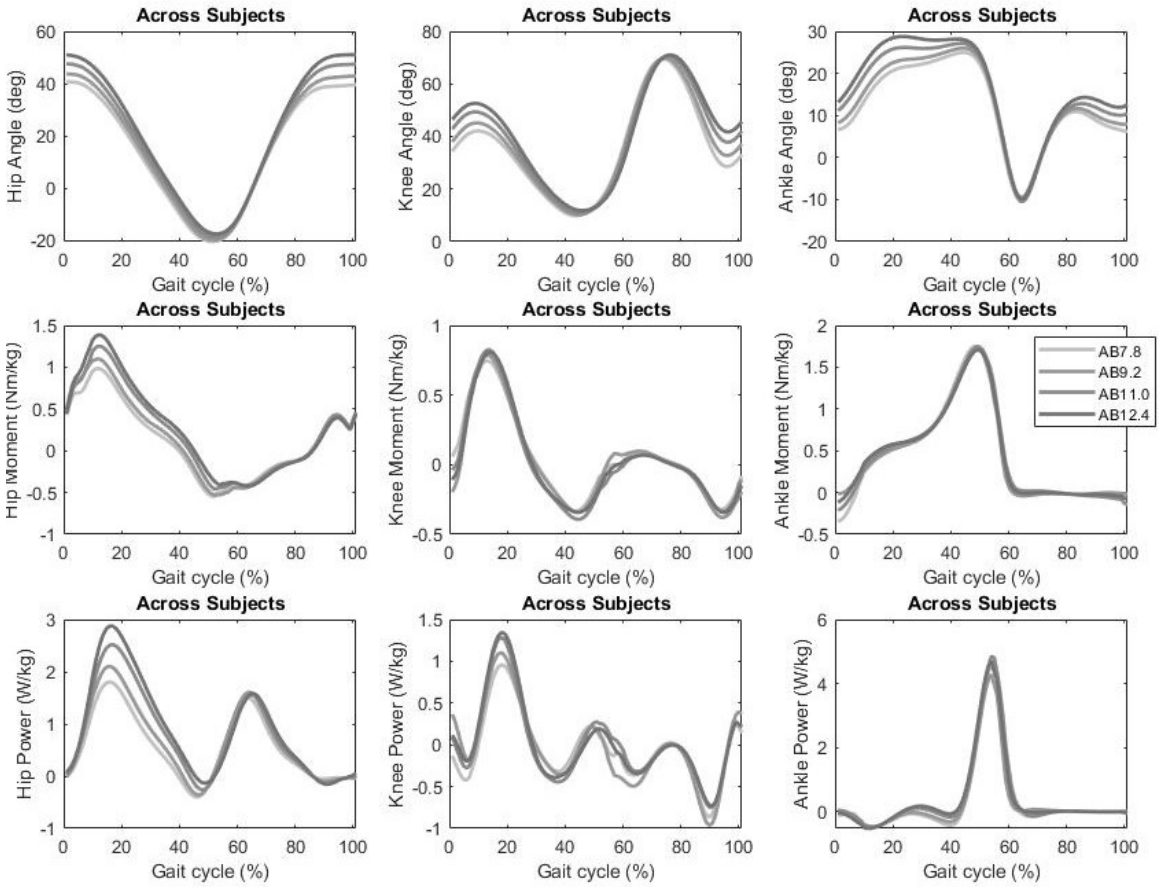

Figure 3.2: AB Knee Biomechanics

3.2.3 Biological Inspired Scaling Equations

In the AB opensource dataset of knee joint during ramp ascent shown in Figure 3.2 [41], the knee initial flexion angle, knee extension moment and knee extension power scales with different context of the ramp inclination angles. Based on the scaling torque profile, this study proposed a linear scaling on the context equation:

$$p_{scaled} = p(1 + \alpha(x - ref)) \tag{3.7}$$

p represents as the impedance parameters used in the impedance controller, and *x*, *ref* represents each current context and reference context of the terrain. In the ramp ascent, the scaled impedance parameter is the stiffness *k* to provide more torque in early stance knee

extension, while in the ramp descent, the scaled impedance parameter is the damping *b* to produce more resistances.

To exhibit the knee initial flexion angle kinematics adaption, this study proposed a linear min-max equation to scale the knee preflexion angle after the Swing Extension phase:

$$\theta = \theta_{nominal} + \frac{(\theta_{max} - \theta_{min})}{(x_{max} - x_{min})}(x - ref) \tag{3.8}$$

and,

$$\theta = \begin{cases} \theta_{max}, & if \theta > \theta_{max}; \\ \theta_{min}, & if \theta < \theta_{min}; \end{cases} \tag{3.9}$$

This equation shows a linear interpolation of the preflexion angle based on the maximum and minimum context values. The initial knee flexion angles are limited by the maximum and minimum output angle values.

The last scaling equation used in this control is to use the a switch velocity equation to break the Early Stance into two phases. The first half of Early Stance used the same equation from Equation 3.5 to scale the stiffness on weight while the second half of Early Stance used the linear scaling on context equation from Equation 3.7. The switch threshold uses the angular velocity of the knee joint:

$$k_s = \begin{cases} C(\frac{F - F_{Initial}}{F_{Initial} - F_{Final}})(k_{s,Initial} - k_{s,Final}) + k_{s,Initial}, & if \dot{\theta}_{knee} < \dot{\theta}_{threshold}; \\ k(1 + \alpha(x - ref)), & if \dot{\theta}_{knee} > \dot{\theta}_{threshold}; \end{cases} \tag{3.10}$$

3.2.4 Experiment Protocol

Individuals with unilateral transfemoral amputation (N=8 active prosthesis subjects and N=5 passive prosthesis subjects, deciphered with the TF subject number, two women and six men, age: 49.63 $\pm$ 16.06 years, mass: 87 $\pm$ 15 kg, height: 1.77 $\pm$ 1.5 cm) provided written informed consent for this study under the Institutional Review Board of the Georgia

Institute of Technology. Subjects performed ramp ascent and descent tasks using the active knee-ankle prosthesis and their own passive prosthesis. For active knee-ankle device, subjects needed to complete a training and tuning session of the impedance parameters based on their comfort and needs. Because the passive prosthesis is used in their daily life and they already acclimated to this device, a tuning and training session was not required for the passive device. Subjects were instructed to conduct five full ramp ascent and descent trials under four slope angle conditions each at 7.8°, 9.2°, 10.8° and 12.4°. The passive prosthesis protocol contains transfemoral subjects who wear their clinically prescribed passive prostheses at the nominal slope configuration of 10.8°. The subjects were asked to perform their normal gait patterns as in daily life. During the data collection session, the subjects were marked up with OSL OpenSim marker set (later explained in Chapter 4) and 3-D motion capture system (Vicon, Oxford, UK) and Bertec Force Plates were used to record the kinematics and GRFs of the subject. A static pose was recorded before performing slope walking for model scaling purposes.

3.3 Results

3.3.1 IK, GRF, ID and JP

The motion capture data underwent a biomechanics pipeline (later explained in the Chapter 4) OpenSim from scaling, to generate inverse kinematics and inverse dynamics. The result shown in Figure 3.4 and Figure 3.5 are generated by averaging throughout all subject trials at each presets. The comparison is made between the AB dataset and each prosthetic and intact limb when subjects wear active prostheses and passive prostheses. In Figure 3.4, the intact joint exhibited almost identical profiles in the inverse kinematics and dynamics of the knee. However, the intact ankle movements and moments shows different performances. Thus, the joint power (JP) of the intact ankle is significantly smaller than AB dataset results. The movement of the intact limbs when the subject wears the passive device does not differentiate from the active devices.

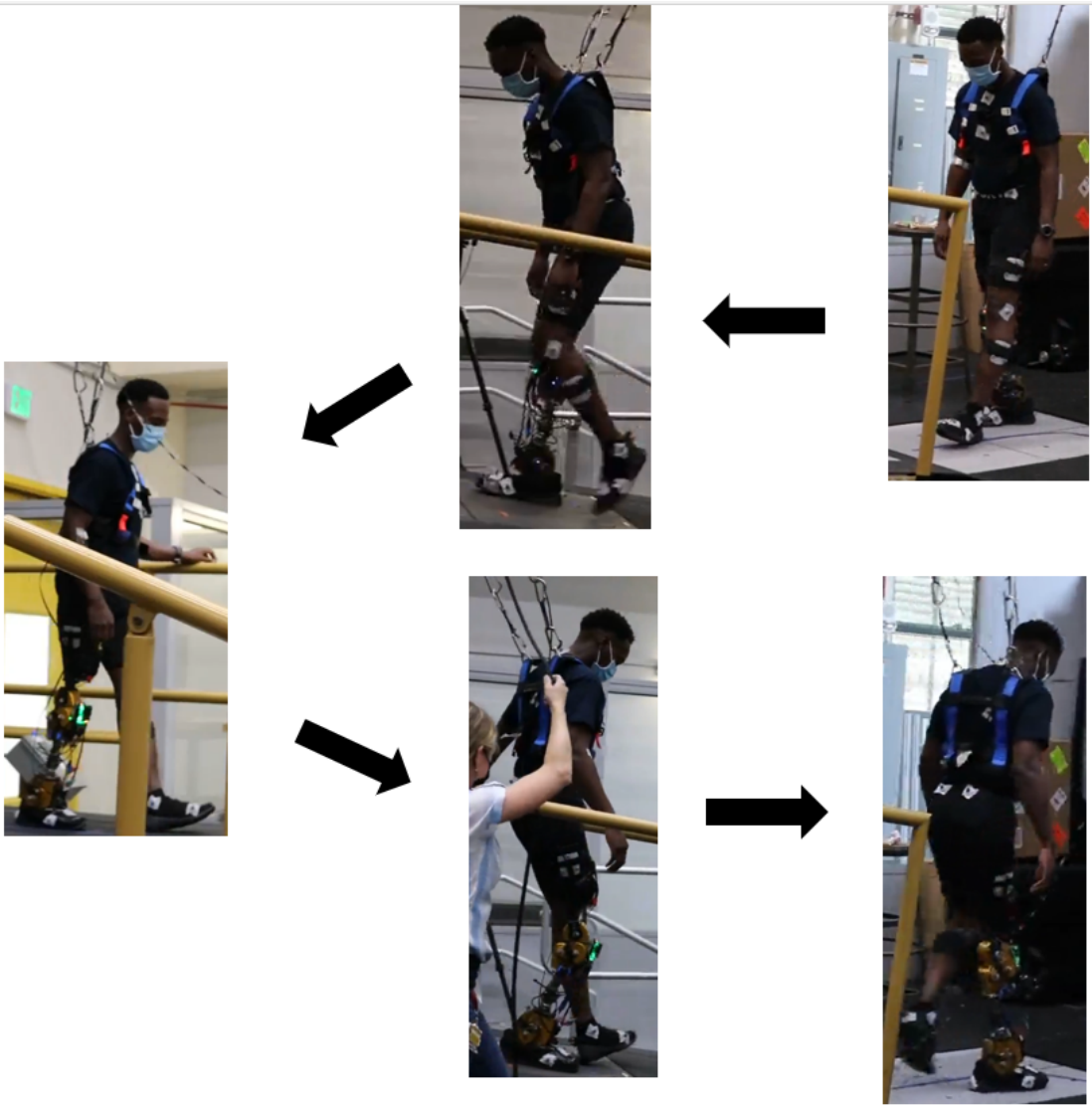

Figure 3.3: Ramp Scaling Controller Protocol

In Figure 3.5, the prosthetic limb indicated large differences compared to the AB dataset. Although the hip kinematics and kinetics implied similar profiles, the knee and ankle joints show no correlations in inverse dynamics and joint power. In all trials, the knee can replicate the pattern of motion of the knee joints of the AB with knee flexion, but the knee moment exerted nearly zero moment and showed no joint power during Early Stance. Meanwhile, the ankle performed like a passive ankle with even a less passive ankle joint torque.

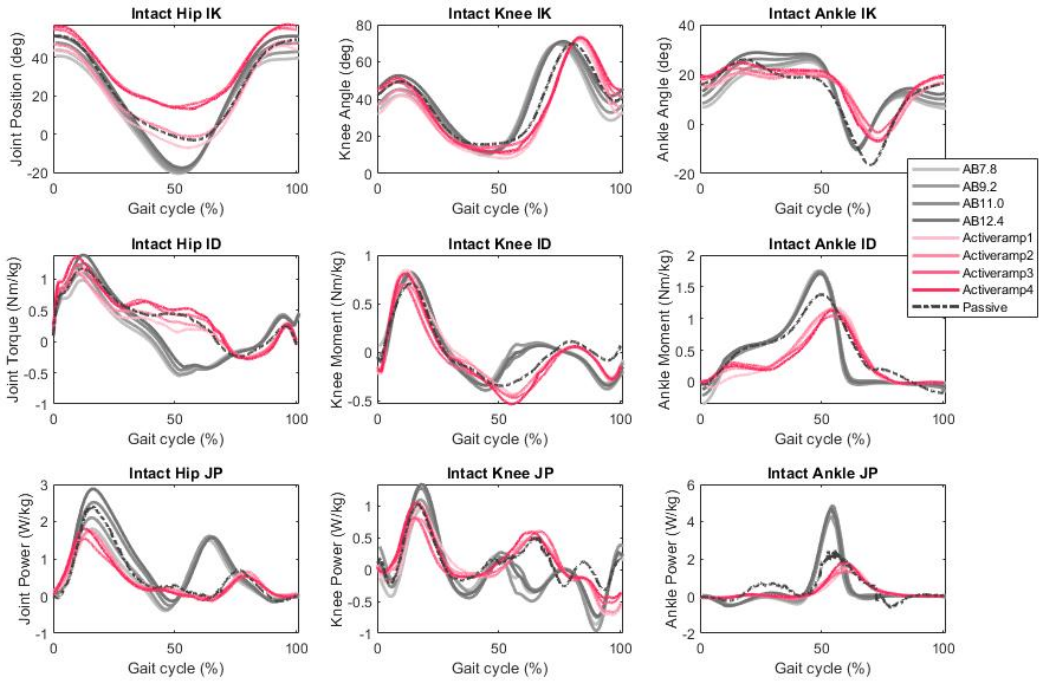

Figure 3.4: Unilateral Transfemoral Amputee Intact Limb side when wearing Active Prosthesis

3.3.2 Energy Expenditure

The positive and negative energy pie chart showing the distribution of energy expenditure when unilateral transfemoral amputees wearing active and passive prosthesis are shown in Figure 3.6. Despite the small positive energy generated by both the active ankle and knee prosthesis, the intact hip energy exerted and the percentage of loading are significantly reduced. In addition, the total energy expenditure of the active prosthesis users is smaller than that of the passive prosthesis users.

In the negative energy expenditure, all joints almost remain the same amount of loading, except the active prosthetic ankle absorbs less energy than the passive ankle prosthesis. In general, active prosthesis users show less energy absorbed than passive prosthesis users.

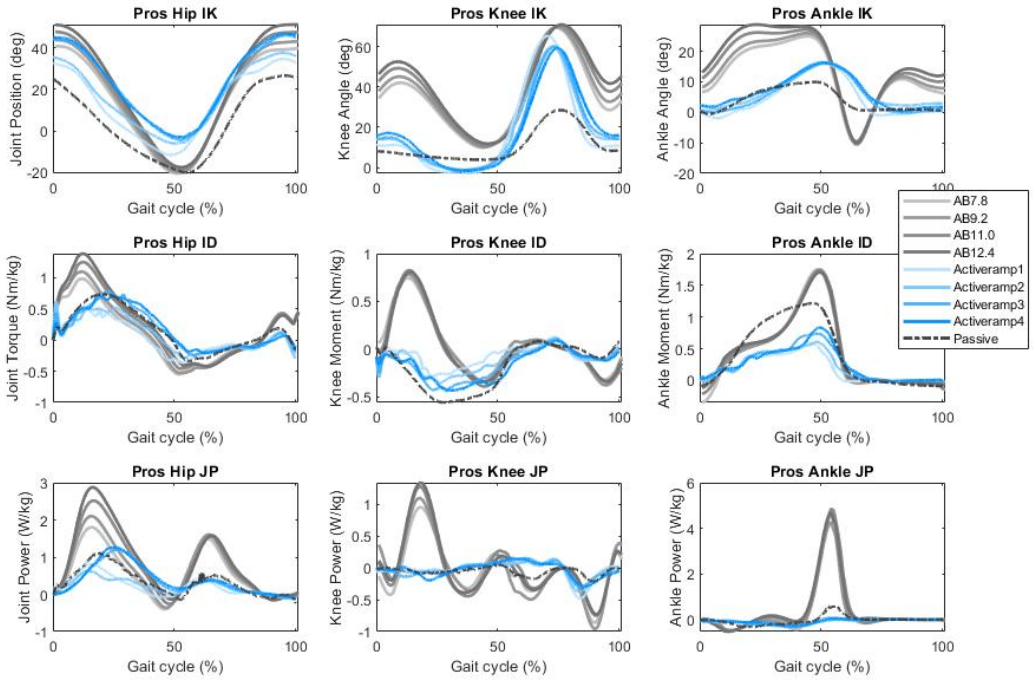

Figure 3.5: Unilateral Transfemoral Amputee Prosthetic Limb side when wearing Active Prosthesis

3.3.3 Handrail Usage and Stride Metrics

In Table 3.2 shows the handrail usages of each subject while wearing the active prosthesis. This metric indicates the percentage of loading on the handrail which represents how much weight was loaded on the powered prosthesis. TF08 showed the highest handrail usage among all other subjects in both ramp ascent and descent. The averaged handrail usages are below 11% of body weight which is an acceptable level of weight loading onto the prosthetic device. The stride metrics is shown in the Table 3.3 which are averaged across all subjects using the active prosthesis on different presets. Subjects tend to spend more time on the intact side than on the prosthetic side in general, except for preset 3. The prosthesis stance time of all presets is significantly lower than intact stance time.

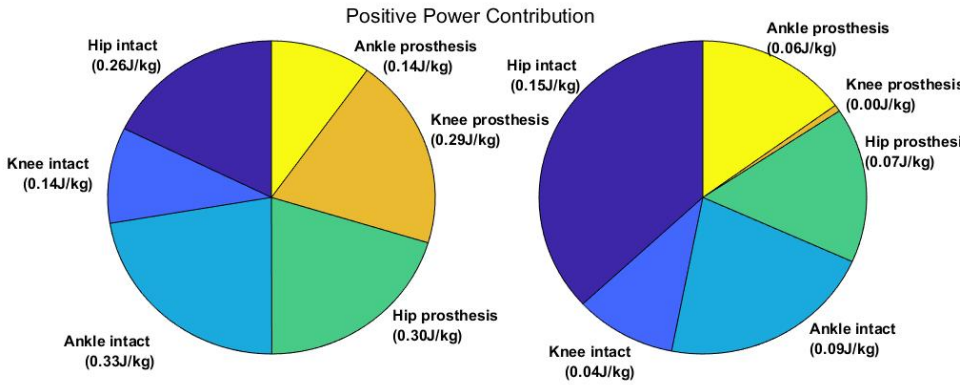

Figure 3.6: Energy Expenditure Pie Chart Among Unilateral Transfemoral Amputee Prosthetic Limb Side when Wearing Active and Passive Prosthesis

Table 3.2: Handrail Usage

	TF02	TF03	TF05	TF07	TF08	TF11	TF12	TF15	Average
Ascent	7.01%	12.56%	3.48%	6.93%	20.04%	16.53%	7.98%	1.77%	9.397%
Descent	8.59%	10.35%	8.33%	11.97%	12.08%	8.41%	7.08%	7.18%	10.27%

3.4 Discussion

Based on all metrics from the results, it is clear that the active prosthetic knee did not generate enough torque to provide early stance knee extension assistance. Meanwhile, the ankle also performed like a passive prosthesis with no active motion in kinematics and essentially no moment generated from the device.

The joint power of the active prosthesis shows even a lower value than that of the passive prosthesis. This indicates that active prosthesis did not work properly at all and acted like a free door hinge. The reason that even passive ankle prosthesis can produce higher positive power than active ankle prosthesis is due to the elastic energy restoration during the late stance. Thus, based on the impedance control equation, the stiffness of the active ankle prosthesis could have been set to none, which would yield zero moments or resistances.

The knee generated some extension torque; however, the prosthetic device did not assist in knee extension. In Figure 3.5, the prosthetic knee moment exerts an extension torque before 20% of the gait cycle. This means that the T1 transition which from Early Stance to

Table 3.3: Stride Metrics (Unit: second)

	Prosthesis Stance	Prosthesis Swing	Prosthesis Total	Intact Stance	Intact Swing	Intact Total
Preset 1	0.8508	0.6426	1.4934	1.0741	0.4452	1.5193
Preset 2	0.8721	0.6276	1.4997	1.0722	0.4493	1.5215
Preset 3	0.9269	0.6203	1.5472	1.0740	0.4307	1.5047
Preset 4	0.9082	0.5747	1.4828	1.0846	0.4692	1.5538
Average	0.8895	0.6163	1.5058	1.0762	0.4486	1.5248

Late Stance phase got triggered earlier than expected. The active prosthesis reached to Late Stance phase before knee extension. During the late stance, the equilibrium knee angle will be no longer zero to fully extend the knee.

Thus, a new controller is needed to prevent these situations from happening. Otherwise, the assistance of an active prosthesis becomes minimal and does not act differently compared to a passive prosthesis.

CHAPTER 4
DEVICE DEVELOPMENT

4.1 Overview

This chapter explains the tools built to assist OSL users with loading the prosthetic device on the scaling smart controller. In the previous chapter, the prosthetic stance time and intact stance time indicated an asymmetric gait on the ramps. This might be due to the trust of the device and improper training on how to load on the OSL. Thus, a sit-to-stand (STS) controller is implemented into the FSM.

4.2 Sit-to-Stand Controller

Simon *et al.* designed an STS controller that is able to transition from Early Stance of walking mode to Stand-to-Sit phase of STS mode using EMG sensory classifiers [51]. This strategy is not used here due to impracticalities associated with implementation of external sensors onto the users. The best solution is to use only the OSL integrated sensor. Varol *et al.* designed a STS controller that can transition from Stand to Sit using the sagittal moment as the threshold. These two strategies showed different methods in transition phases. Varol *et al.* modulated the stiffness as a function of knee angle for both stand-to-sit and sit-to-stand phases. Simon *et al.* applied different methods to each transition phase. In the stand-to-sit phase, a damping equation is used, which is demonstrated in Chapter 3 Equation 3.4. This equation will change the knee equilibrium angle that is always smaller than the current angle reading. Such a strategy will turn the knee into a passive damper to provide resistances to the user while stand-to-sit. In the sit-to-stand phase, a scale-on-weight equation which is also demonstrated in Chapter 3 Equation 3.5 is used to provide knee extension during sit-to-stand. Since the purpose of the STS controller for our study is to teach

a subject how to load on the knee, the transition phases control from Simon *et al.* are used in our study. Thus, a combination of both STS controller are implemented into the FSM to the OSL.

In general, the STS mode in FSM was set as the same structure as the other modes. The STS mode has four phases and four transitions. The knee and ankle joint can be set as the same equations throughout the phases. When the subject is in the standing phase, the subject can trigger the T1 transition by actively bending both knees to generate a sagittal moment. Once this sagittal moment exceeds the threshold value measured by the 6-DOF loadcell, it will transit to Stand-to-Sit phase. During this phase, the subject is able to bend the knee with resistance provided by the actuators to prevent falling, and slowly reach the sitting phase when the knee reaches an angle threshold. During the sit phase, the knee will act like a hinge on the free door without any resistance or assistance. If the subject wants to stand up, the subject has to actively load both lower limbs to reach the vertical force threshold to trigger T3 transition. Then the OSL will be in Sit-to-Stand phase where prosthetic knee and ankle will provide extension assistance to stand without overly exerting the intact limb.

In the next iterations of ramp scaling controller testing, the subject will be asked to perform STS motion multiple times until the subject is comfortable enough and seamlessly triggers the transitions. This process can help users learn how to load the knee to trigger transitions not only in the STS mode, but also in other modes such as Ramp Ascent.

4.3 Graphical User Interface

To run the STS mode from FSM, a new Graphical User Interface (GUI) is designed and implemented with new features for better real-time and off-time control. In the GUI, the user can change the impedance parameters and control the switching modes. At the same time, each impedance parameter can be changed to associate any equations if needed. Thus, when STS controller is used, and if the subject might feel Sit-to-Stand phase assistance too

small, the GUI can increase the stiffness at those phases starting from the next round of phase. The GUI can also detect the real-time context published into the ROS service, and the user can monitor the context simultaneously.

4.4 DENEB Pipeline

For a smoother and easier generation of biomechanical data, an automated biomechanics pipeline, Dynamic Examination aNd Evaluation of Biomechanics (DENEB), is designed and built to retrieve information on inverse kinematics and inverse dynamics at each joints. The OpenSim model is modified from the baseline model, gait2354, and the prosthetic body segments are replaced with OSL parts. The new modified model can be used to perform a full-body biomechanical analysis from motion capture and GRF data. In the same fashion, a modified model for passive prosthesis is utilized for passive full-body biomechanics analysis.

4.4.1 OpenSim OSL model

The OpenSim model version of the OSL is designed as an opensource model. Currently, OSL is used in several different research collaborations. All groups have built and studied on the same version of knee-and-ankle prosthesis. One of the most important methods for measuring the outcome of the prosthesis is to compute human biomechanics during walking. This requires musculoskeletal models as the baseline model to compute the user's biomechanical information at the joint, muscle, and tendon level. Although the powered robotics prosthesis can be collaborated with all sensor data, in-depth human biomechanical information such as joint inverse kinematics and inverse dynamics are still unknown without thorough biomechanical analysis. Onboard sensors can only render the sensor information which might not represent user's biological behavior. Modeling prosthetic devices similar to human morphology also may not yield an accurate representation of the human and device interaction. Using human limb segments to emulate OSL performance

may not yield an accurate result. There is also no existing OSL model with OpenSim for all other research collaborations using this type of device for biomechanical analysis

The OSL model designed consists of two housings, one for the knee assembly and the other for the ankle assembly. DriveOutputKF represents as the knee joint center while ShanktoFoot represents as the ankle joint center. These two locations will be used as the joint center to estimate the inverse kinematics and dynamics of the knee and ankle. The pylon is located between these two assemblies and the length can be adjusted by the scaling tool. There are two versions of the model where the only difference is that the side of the prosthesis is mirrored. Currently the marker set used in this model involves four markers for the torso, four markers for pelvis, three markers for each thigh and the intact shank, two markers for each knee joints and the intact ankle, and finally four markers for each foot. The markers on the OSL are set at the center of each gear set. Scaling, inverse kinematics and inverse dynamics are computed using these models in OpenSim with MoCapTools toolbox [53]. The biomechanics pipeline is generated with time-series data of joint kinematics, torque, and power.

4.4.2 Model Validation

Experiment Protocol

To validate the quality of the OSL model, experiments with N=4 individuals with unilateral amputation (3 men + 1 woman, age: 60.75 $\pm$ 10.63 years, height: 1.76 $\pm$ 0.17 m, mass: 78.0 $\pm$ 14.4kg, pylon height: 10.3 $\pm$ 8.1 cm) were performed with Vicon's motion capture system to track marker trajectories and asked the subject to walk at a constant walking speed of 0.8m/s.

At the beginning of the experiment, the subject is fit with the OSL and trained to walk within the handrails. Following the tuning procedure and when the subject is comfortable ambulating, the marker set is applied to the subject. Before walking on the treadmill, the subject will be asked to complete a static pose recording. This static pose trial is designated

for the scaling tool in the OpenSim. Subsequently, the subject will walk on the treadmill. The OpenSim OSL model pipeline used the same workflows stated in Chapter 2: Static workflow and Inverse Kinematics workflow.

Validation: Model Kinematics RMSE

To validate the accuracy of the results using the OSL Opensim model, the inverse kinematics data of two joints, which are knee and ankle, with the two joint encoder readings are compared. The angle RMSE for all subjects shows all values under 5 deg difference. After averaging the results across all subjects, the knee reported an average of 2.34 deg with 0.44 deg standard deviation. The ankle exhibits an average of 2.54 deg difference with 0.58 deg standard deviation. Both results correspond to a difference of 1.95% and 8.46% of the range of motion. Based on the report of opensim office results, any result below 5 deg RMSE demonstrates a good to acceptable level.

Conclusion

In conclusion, this study released unilateral generic models for both the left and right sides. At the same time, it provided the markers sets and the scaling method to adjust the length of the pylon according to the prosthesis accordingly. Finally, this study validated the joint-level kinematics in comparison to the onboard OSL sensors. In future work, there is still development needed in building Inverse dynamics workflow in the Opensim. The inverse dynamics tool can generate joint load information for better understanding of the biological torque at the joint level. Similarly, modeling of dynamic effects between the residual limb and the socket interface also affects the biomechanics outcome. An accurate and thorough biomechanics analysis can be done with all these factors considered in the modeling.

CHAPTER 5
ITERATED RAMP SCALING WALKING STUDY

5.1 Methodology

5.1.1 Controller Modification

The previous study in Chapter 4 indicated the scaling equations did not work. This may indicate that the focus of the scaling effect is wrong.

Originally the controller focused on scaling the knee moment on different presets. However, when taking a closer look at the kinematics, kinetics and joint power of the knee shown in Figure 3.2, the dominant scaling effect in joint power is the result of change in kinematics instead of kinetics. If only the first 60% of gait cycle is examined in kinematics, the knee joint enters Early Stance with significant scaling effect of initial flexion angle and increase the knee flexion until around 10% of gait cycle. From 10% to 45% of the gait cycle, the knee joint will extends to -20° for all contexts. Then around 45% of the gait cycle, the knee should enter Late Stance phase and by this moment the knee should be at Early Stance. When taking a closer look at the knee kinematics, the first 10% of the gait cycle show that the knee generates a flexion torque that is not needed among transfemoral individuals, as the controller does not actively bend on them. From 10% to 45% of the gait cycle, knee will exert a large extension torque with small scaling effects. Thus, in knee joint power, a great scaling effect can be seen from 20% to 35% of gait cycle. This means the smart scaling controller should focus on scaling the kinematic changes in the knee flexion while provide small scaling effect on the knee torque. The original Equation 3.10 changes the stiffness from scaleOnWeight to scaleOnContext, while the equilibrium knee angle uses the scaleOnWeight equation from the previous flexion angle to zero. There are three problems in these previously proposed scaling equations: 1) the switch flag of the equation is to

alter the stiffness such that the knee extension torque scales with higher stiffness value. The switch flag uses the knee velocity as the threshold, but the knee velocity did not align with the subject load information. If the knee velocity threshold was reached, but the subject did not load on the prosthetic knee, the prosthesis will expand with a significantly smaller motor and biological torque. Thus, a better switch method is needed such as the switch weight threshold. This threshold can use the percentage of the weight the user spent on the device and change the stiffness to extend the knee when they have properly loaded the device. 2) The first half of the equation is to allow the user to slightly increase the angle of flexion and then extend the knee with additional flexion. The stiffness during the first half of the equation was never set lower enough to allow users to bend in addition. The second half of stiffness should start with the previous value in the first half and then scale to a final value without an instant increase in the motor torque commanded. This can be fixed by changing the first half of Early Stance phase stiffness to a small value that allows the user to bend the knee properly and uses ScaleOnWeightEqn in the second half of the phases to gradually increase the stiffness value. 3) The knee equilibrium angle was not set properly. Using the scale-on-weight equation, the initial value of the angle matched with the preflexion angle, but the final value was set to zero and changes based on the weight loaded on the device. If the user cannot bend the knee with additional angle, based on the impedance parameter equation, the desired torque will be an extremely small value regardless of the stiffness value when current knee angles keeps matching with desired angles. This can be fixed by setting the knee equilibrium angle to zero throughout the entire Early Stance phase. Thus, the more the prosthetic knee joint bends, the more torque will be generated to match the intact knee joint.

The effect of the ankle joint kinematics affects the control substantially as well. The original T1 transition from Early Stance to Late Stance uses only ankle angle as the threshold. In the kinematics of the level walking ankle, the ankle does not reach maximum dorsiflexion until 45% of the gait cycle. Thus, the ankle T1 threshold would never be

miss-triggered during level walking. However, in ramp ascent kinematics, the ankle angle tends to reach max dorsiflexion earlier with higher inclination angle. This will cause the T1 miss-trigger and lose the ability to generate the knee extension assistance in the Late Stance phase. Without adding additional threshold to T1 transition, the T1 ankle threshold should also scales with the context. Due to the limitation of the range of motion in the ankle part, the maximum dorsiflexion only reaches 20°. Thus, another compensatory strategy is used in the controller. Besides increasing the T1 threshold, the ankle stiffness is also increased to prevent reaching the first peak of two bumps showing in the AB kinematics data.

5.1.2 Experiment Protocol

The experiment data was only tested and processed using one AB subject wearing an AB adaptor (*iWalk*). The subject is asked to walk on the treadmill at four different angles of inclination. The subject is marked up with the same marker set from previous chapter and motion capture system and force plates are used to record the marker trajectory and GRFs data. Subjects walked on the treadmill for 30 seconds for each slope condition.

5.2 Results

Figure 5.1 shows the inverse kinematics, inverse kinetics, GRF, and joint power results of both the prosthetic and the intact side. Both prosthetic and the intact limbs show distinct differences from the AB dataset, which could be due to the usage of the AB adaptor, but the subject exhibited similar profiles in two lower limbs. In the hip joint, both hip kinematics and kinetics shows almost identical profiles. In the knee joint, the prosthetic side shows a wider range of motion than the intact side. Both limbs are able to demonstrate a scaling effect of preflexion on different context. In inverse kinematics, both limbs are also able to produce flexion resistance in the first half of Early Stance and knee extension torque in the second half of phase. Also, it is apparent that the torque profiles scaled slightly as inclination angle increased. The joint power of the knee shows the greatest scaling effect

in the Early Stance phase. In the ankle joint, the inverse kinetics of the prosthetic ankle matches with the intact side. This indicates that the prosthetic ankle joint can generate extension assistance during slope walking compared to the previous chapter. However, the joint power plot still indicates the missing power of prosthetic ankle side.

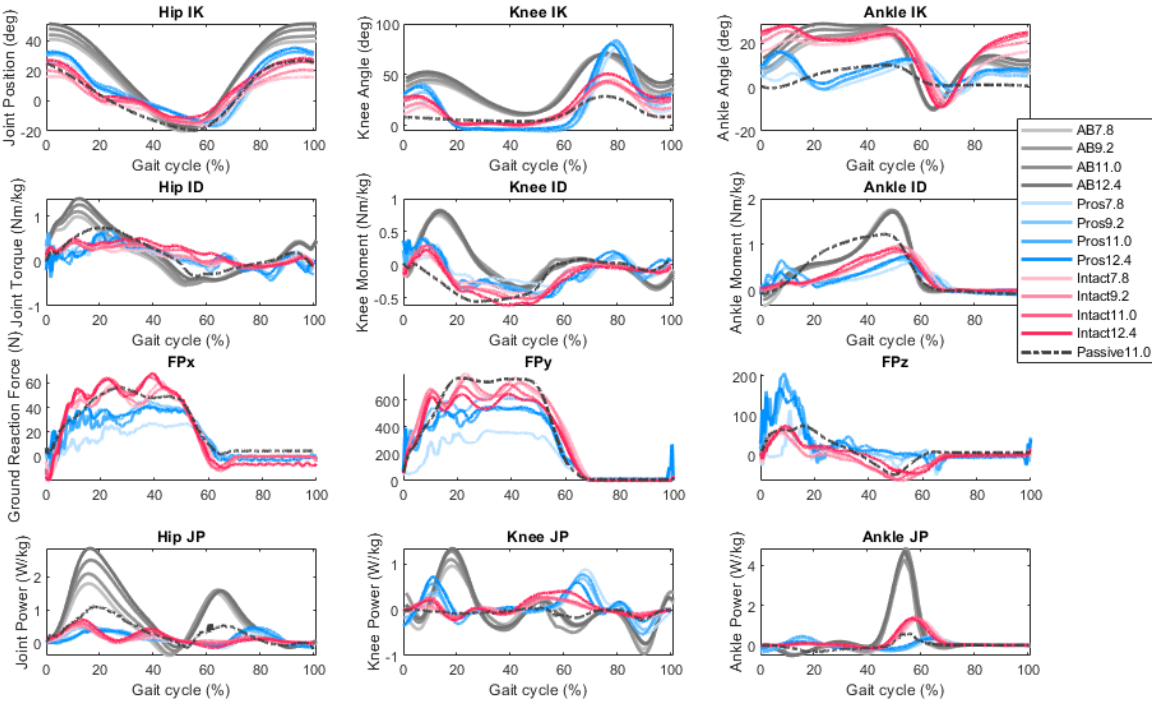

Figure 5.1: Knee Prosthetic and Intact Limb Biomechanics with AB Adaptor

Figure 5.2 shows the stride metrics of the subject with the AB wearing a powered prosthesis using the AB adaptor. Stance time, swing time, and total stride time show a symmetric gait at all different presets. Although this is an AB subject data, it may be indicative of the ability to restore gait symmetry for individuals with unilateral transfemoral amputation users.

5.3 Discussion

The result generated from the AB subject data shows a decent scaling effect of knee kinematics in initial flexion angle and additional flexion, knee kinetics in knee extension moment and joint power. This indicate the controller is able to render the scaling effects

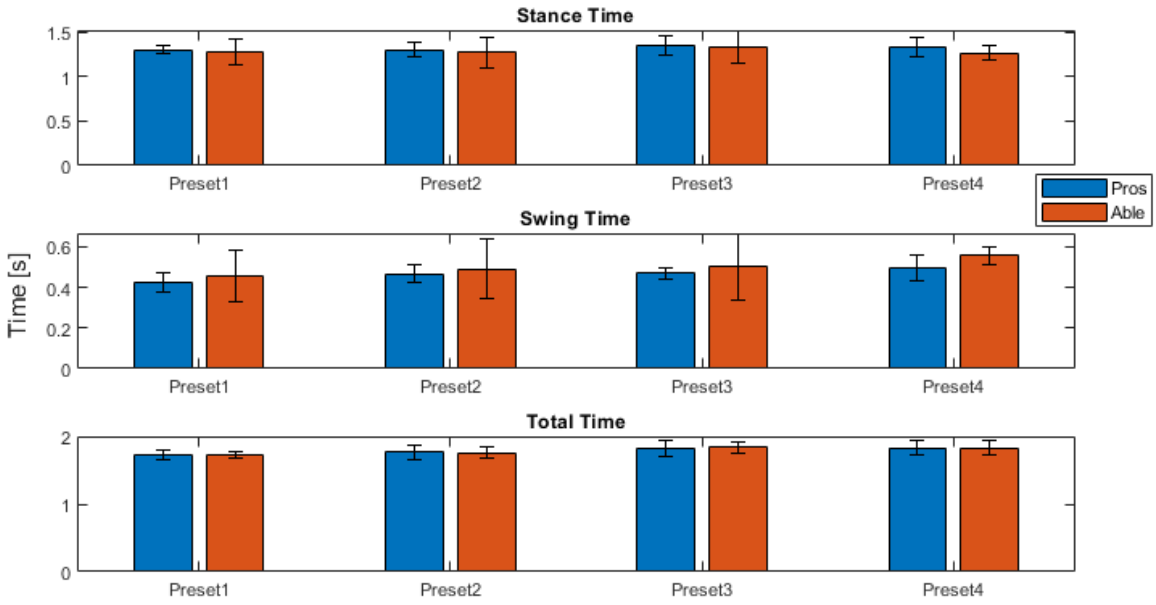

Figure 5.2: Stride Metrics with AB Adaptor

especially on the knee joint in ramp ascent. However, replicating the same result in users of unilateral transfemoral powered prostheses is still challenging. Based on the feedback of most users, the initial flexion angle intimidated them to place the limb with proper step length. Also, trusting the device affects the amount of loading to the device. These psychological effects should all be considered into the training session.

Although the controller demonstrated a good result for an AB subject, there are still other factors to consider to further improve the performance of the controller. In the joint kinematics, the knee equilibrium angle is always set to zero. This means that the controller cannot control the amount of additional flexion angle in the first half of the bending phase. To avoid miss-triggering transitions from Early Stance to Late Stance, there should be more than one parameter and more than one ankle angle threshold into the FSM.

CHAPTER 6
DISCUSSION AND CONCLUSION

6.1 Narrowing Beam Walking Test Balance Study

From the evaluation of the balance study on the narrowing beam walking test of two subjects, we see a general performance distinction between different MPKs. Cleg performs the worst among all three MPKs in either the regulation of WBAM or the distance traveled on the NBWT. RheoKnee and PowerKnee showed similar results in distance metrics, but with unstable WBAM regulations. All three MPKs are built with unique knee stance flexion control features. This feature can be correlated with the performance when walking on the beam and the regulation of WBAM. All three MPKs show a distinctive difference between the WBAM of the falling event and the WBAM of the other gait cycles, especially in frontal plane. Peak-to-peak values are evaluated with each segment of the beam to distinguish the performance of WBAM regulation with each MPK. Foot Placement was implied as the main cause of falling during the beam walking. Challenges arise when MPK users encounter a narrower step width or a smaller contact surface area due to loss of proprioception of the foot. Foot misplacement can cause the COM to accelerate vertically down. The threshold in the frontal WBAM to detect the falling event cannot be quantified yet.

6.2 Iterated Ramp Scaling Walking Study

Inspired by the biomechanics of the AB subjects, the initial knee flexion angle, the knee extension moment, and the knee extension power scales with different context of the ramp inclination angles. To render similar profiles, a linear scaling on context equation, a linear min-max equation to scale the knee preflexion angle after the Swing Extension phase, and a switch velocity equation to break the Early Stance into two phases are used. For the

ramp scaling walking test, the active prosthetic knee and ankle did not generate sufficient torque to provide Early Stance knee extension assistance on the ramp in initial tests. The joint power of the active prosthesis shows an even lower value than that of the passive prosthesis.The active prosthesis did not work properly and acted like a hinge on a free door. Before the next benchtop test, development tools were built to help users better adapt to the device. A STS controller is implemented into the FSM and GUI. In this study, an open-source OpenSim OSL model is also designed and validated. In the iterated ramp-scaled walking study, the controller is designed using a different approach to scale the kinematics instead of the kinetics of the knee joint. In the knee joint, the prosthetic side shows a wider range of motion than the intact side. Both limbs are able to demonstrate a scaling effect of preflexion on different context. In inverse kinematics, both limbs are also capable of producing flexion resistance in the first half of the Early Stance and knee extension torque in the second half of the phase. The joint power of the knee shows the greatest scaling effect in the Early Stance phase. In the ankle joint, the inverse kinetics of the prosthetic ankle matches with the intact side. Although the controller demonstrated a good result for an AB subject, there are still other factors to consider to improve the performance of the controller. In the joint kinematics, the knee equilibrium angle is always set to zero. This means that the controller cannot control the amount of additional flexion angle in the first half of the bending phase. To avoid miss-triggering transitions from Early Stance to Late Stance, there should be more than one parameter and more than one ankle angle threshold set in the FSM.

6.3 Limitation and Future Work

The main limitation of this study is the number of participants. The goal of NBWT study is to recruit 10 individuals with unilateral transfemoral amputation subjects in total, and each subject's total experiment time will be at least four weeks. Developing methods to collect GRFs for inverse kinetics measurement during the NBWT will provide a better

understanding of joint loads during this challenging task. The OSL scaling experiment only validated the result using the AB adapter. A formal test is needed from actual transfemoral prosthesis users to fully validate controller performance. For future work, a similar scaling effect is needed on ramp descent damping control. Finally, the development of an ankle ramp scaling controller can be beneficial for individuals with transfemoral amputation.

REFERENCES

[1] K. Ziegler-Graham, E. J. MacKenzie, P. L. Ephraim, T. G. Travison, and R. Brookmeyer, "Estimating the prevalence of limb loss in the United States: 2005 to 2050," *Archives of Physical Medicine and Rehabilitation*, vol. 89, no. 3, pp. 422–429, Mar. 2008.

[2] I. C. Narang, B. P. Mathur, P. Singh, and V. S. Jape, "Functional capabilities of lower limb amputees," *Prosthetics and Orthotics International*, vol. 8, no. 1, pp. 43–51, Apr. 1984.

[3] W. S. Li, S. Y. Chan, W. W. Chau, S.-W. Law, and K. M. Chan, "Mobility, prosthesis use and health-related quality of life of bilateral lower limb amputees from the 2008 Sichuan earthquake," *Prosthetics and Orthotics International*, vol. 43, no. 1, pp. 104–111, Feb. 2019.

[4] J. P. Pell, P. T. Donnan, F. G. Fowkes, and C. V. Ruckley, "Quality of life following lower limb amputation for peripheral arterial disease," *European Journal of Vascular Surgery*, vol. 7, no. 4, pp. 448–451, Jul. 1993.

[5] K. A. Ingraham, N. P. Fey, A. M. Simon, and L. J. Hargrove, "Assessing the Relative Contributions of Active Ankle and Knee Assistance to the Walking Mechanics of Transfemoral Amputees Using a Powered Prosthesis," *PloS One*, vol. 11, no. 1, e0147661, 2016.

[6] E. Chiovetto, M. E. Huber, D. Sternad, and M. A. Giese, "Low-dimensional organization of angular momentum during walking on a narrow beam," *Scientific Reports*, vol. 8, p. 95, Jan. 2018.

[7] A. H. Shultz, J. E. Mitchell, D. Truex, B. E. Lawson, and M. Goldfarb, "Preliminary evaluation of a walking controller for a powered ankle prosthesis," in *2013 IEEE International Conference on Robotics and Automation*, ISSN: 1050-4729, May 2013, pp. 4838–4843.

[8] F. Sup, H. A. Varol, and M. Goldfarb, "Upslope Walking With a Powered Knee and Ankle Prosthesis: Initial Results With an Amputee Subject," *IEEE Transactions on Neural Systems and Rehabilitation Engineering*, vol. 19, no. 1, pp. 71–78, Feb. 2011, Conference Name: IEEE Transactions on Neural Systems and Rehabilitation Engineering.

[9] R. Riener, M. Rabuffetti, and C. Frigo, "Stair ascent and descent at different inclinations," *Gait & Posture*, vol. 15, no. 1, pp. 32–44, Feb. 2002.

[10] E. D. Ledoux and M. Goldfarb, "Control and Evaluation of a Powered Transfemoral Prosthesis for Stair Ascent," *IEEE Transactions on Neural Systems and Rehabilitation Engineering*, vol. 25, no. 7, pp. 917–924, Jul. 2017, Conference Name: IEEE Transactions on Neural Systems and Rehabilitation Engineering.

[11] B. E. Lawson, H. A. Varol, A. Huff, E. Erdemir, and M. Goldfarb, "Control of Stair Ascent and Descent With a Powered Transfemoral Prosthesis," *IEEE Transactions on Neural Systems and Rehabilitation Engineering*, vol. 21, no. 3, pp. 466–473, May 2013, Conference Name: IEEE Transactions on Neural Systems and Rehabilitation Engineering.

[12] S. GANGULI, K. S. BOSE, S. R. DATTA, B. B. CHATTERJEE, and B. N. ROY, "Ergonomics Evaluation of Above-Knee Amputee-Prosthesis Combinations," *Ergonomics*, vol. 17, no. 2, pp. 199–210, Mar. 1974, Publisher: Taylor & Francis _eprint: https://doi.org/10.1080/00140137408931339.

[13] M. E. Dewar and G. Judge, "Temporal asymmetry as a gait quality indicator," *Medical and Biological Engineering and Computing*, vol. 18, no. 5, pp. 689–693, Sep. 1980.

[14] K. E. Zelik *et al.*, "Systematic variation of prosthetic foot spring affects center-of-mass mechanics and metabolic cost during walking," *IEEE transactions on neural systems and rehabilitation engineering : a publication of the IEEE Engineering in Medicine and Biology Society*, vol. 19, no. 4, pp. 411–419, Aug. 2011.

[15] V. N. M. Arelekatti and A. G. Winter, "Design of a fully passive prosthetic knee mechanism for transfemoral amputees in India," in *2015 IEEE International Conference on Rehabilitation Robotics (ICORR)*, ISSN: 1945-7901, Aug. 2015, pp. 350–356.

[16] D. Berry, "Microprocessor Prosthetic Knees," *Physical Medicine and Rehabilitation Clinics*, vol. 17, no. 1, pp. 91–113, Feb. 2006, Publisher: Elsevier.

[17] W. Cao, H. Yu, W. Chen, Q. Meng, and C. Chen, "Design and Evaluation of a Novel Microprocessor-Controlled Prosthetic Knee," *IEEE Access*, vol. 7, pp. 178 553–178 562, 2019, Conference Name: IEEE Access.

[18] J. Thiele, B. Westebbe, M. Bellmann, and M. Kraft, "Designs and performance of microprocessor-controlled knee joints," *Biomedizinische Technik/Biomedical Engineering*, vol. 59, no. 1, pp. 65–77, Feb. 2014, Publisher: De Gruyter Section: Biomedical Engineering / Biomedizinische Technik.

[19] B. G. A. Lambrecht and H. Kazerooni, "Design of a semi-active knee prosthesis," in *2009 IEEE International Conference on Robotics and Automation*, ISSN: 1050-4729, May 2009, pp. 639–645.

[20] J. Park, G.-H. Yoon, J.-W. Kang, and S.-B. Choi, "Design and control of a prosthetic leg for above-knee amputees operated in semi-active and active modes," *Smart Materials and Structures*, vol. 25, no. 8, p. 085 009, Jul. 2016, Publisher: IOP Publishing.

[21] Z. Safaeepour, A. Eshraghi, and M. Geil, "The effect of damping in prosthetic ankle and knee joints on the biomechanical outcomes: A literature review," *Prosthetics and Orthotics International*, vol. 41, no. 4, pp. 336–344, Aug. 2017.

[22] A. J. Young and D. P. Ferris, "State of the Art and Future Directions for Lower Limb Robotic Exoskeletons," *IEEE Transactions on Neural Systems and Rehabilitation Engineering*, vol. 25, no. 2, pp. 171–182, Feb. 2017, Conference Name: IEEE Transactions on Neural Systems and Rehabilitation Engineering.

[23] A. J. Young, L. H. Smith, E. J. Rouse, and L. J. Hargrove, "Classification of simultaneous movements using surface EMG pattern recognition," *IEEE Transactions on Biomedical Engineering*, vol. 60, no. 5, pp. 1250–1258, 2012, Publisher: IEEE.

[24] A. J. Young, A. M. Simon, N. P. Fey, and L. J. Hargrove, "Intent recognition in a powered lower limb prosthesis using time history information," *Annals of biomedical engineering*, vol. 42, no. 3, pp. 631–641, 2014, Publisher: Springer.

[25] F. Sup, H. A. Varol, J. Mitchell, T. Withrow, and M. Goldfarb, "Design and control of an active electrical knee and ankle prosthesis," in *2008 2nd IEEE RAS EMBS International Conference on Biomedical Robotics and Biomechatronics*, ISSN: 2155-1782, Oct. 2008, pp. 523–528.

[26] L. J. Hargrove *et al.*, "Robotic leg control with EMG decoding in an amputee with nerve transfers," *New England Journal of Medicine*, vol. 369, no. 13, pp. 1237–1242, 2013, Publisher: Mass Medical Soc.

[27] K. Bhakta, J. Camargo, P. Kunapuli, L. Childers, and A. Young, "Impedance Control Strategies for Enhancing Sloped and Level Walking Capabilities for Individuals with Transfemoral Amputation Using a Powered Multi-Joint Prosthesis," *Military Medicine*, vol. 185, no. Supplement_1, pp. 490–499, Jan. 2020.

[28] E. J. Rouse, L. M. Mooney, and H. M. Herr, "Clutchable series-elastic actuator: Implications for prosthetic knee design," *The International Journal of Robotics Research*, vol. 33, no. 13, pp. 1611–1625, Nov. 2014, Publisher: SAGE Publications Ltd STM.

[29] F. Sup, H. A. Varol, J. Mitchell, T. J. Withrow, and M. Goldfarb, "Preliminary Evaluations of a Self-Contained Anthropomorphic Transfemoral Prosthesis," *IEEE/ASME transactions on mechatronics: a joint publication of the IEEE Industrial Electronics Society and the ASME Dynamic Systems and Control Division*, vol. 14, no. 6, pp. 667–676, 2009.

[30] D. A. Winter, "Biomechanics of Normal and Pathological Gait," *Journal of Motor Behavior*, vol. 21, no. 4, pp. 337–355, Dec. 1989, Publisher: Routledge _eprint: https://doi.org/10.1080/00222895.1989.10735488.

[31] K. R. Kaufman, S. Frittoli, and C. A. Frigo, "Gait asymmetry of transfemoral amputees using mechanical and microprocessor-controlled prosthetic knees," *Clinical Biomechanics (Bristol, Avon)*, vol. 27, no. 5, pp. 460–465, Jun. 2012.

[32] N. T. Pickle, J. M. Wilken, J. M. A. Whitehead, and A. K. Silverman, "WHOLE-BODY ANGULAR MOMENTUM DURING SLOPED WALKING USING PASSIVE AND POWERED LOWER-LIMB PROSTHESES," *Journal of biomechanics*, vol. 49, no. 14, pp. 3397–3406, Oct. 2016.

[33] L. A. Nolasco, A. K. Silverman, and D. H. Gates, "Whole-body and segment angular momentum during 90-degree turns," *Gait & Posture*, vol. 70, pp. 12–19, May 2019.

[34] A. K. Silverman, J. M. Wilken, E. H. Sinitski, and R. R. Neptune, "Whole-body angular momentum in incline and decline walking," *Journal of Biomechanics*, vol. 45, no. 6, pp. 965–971, Apr. 2012.

[35] A. K. Silverman, R. R. Neptune, E. H. Sinitski, and J. M. Wilken, "Whole-body angular momentum during stair ascent and descent," *Gait & Posture*, vol. 39, no. 4, pp. 1109–1114, Apr. 2014.

[36] M. Popovic, A. Hofmann, and H. Herr, "Angular momentum regulation during human walking: Biomechanics and control," in *IEEE International Conference on Robotics and Automation, 2004. Proceedings. ICRA '04. 2004*, ISSN: 1050-4729, vol. 3, Apr. 2004, 2405–2411 Vol.3.

[37] A. K. Silverman and R. R. Neptune, "Differences in whole-body angular momentum between below-knee amputees and non-amputees across walking speeds," *Journal of Biomechanics*, vol. 44, no. 3, pp. 379–385, Feb. 2011.

[38] S. D'Andrea, N. Wilhelm, A. K. Silverman, and A. M. Grabowski, "Does Use of a Powered Ankle-foot Prosthesis Restore Whole-body Angular Momentum During Walking at Different Speeds?" *Clinical Orthopaedics and Related Research®*, vol. 472, no. 10, pp. 3044–3054, Oct. 2014.

[39] M. Pijnappels, M. F. Bobbert, and J. H. van Dieën, "Contribution of the support limb in control of angular momentum after tripping," *Journal of Biomechanics*, vol. 37, no. 12, pp. 1811–1818, Dec. 2004.

[40] M. M. Ankaralı, S. Sefati, M. S. Madhav, A. Long, A. J. Bastian, and N. J. Cowan, "Walking dynamics are symmetric (enough)," *Journal of The Royal Society Interface*, vol. 12, no. 108, p. 20 150 209, Jul. 2015, Publisher: Royal Society.

[41] J. Camargo, A. Ramanathan, W. Flanagan, and A. Young, "A comprehensive, open-source dataset of lower limb biomechanics in multiple conditions of stairs, ramps, and level-ground ambulation and transitions," *Journal of Biomechanics*, vol. 119, p. 110 320, Apr. 2021.

[42] A. Sawers and B. Hafner, "Validation of the Narrowing Beam Walking Test in Lower Limb Prosthesis Users," *Archives of Physical Medicine and Rehabilitation*, vol. 99, no. 8, 1491–1498.e1, Aug. 2018.

[43] M. J. Major, S. Fatone, and E. J. Roth, "Validity and Reliability of the Berg Balance Scale for Community-Dwelling Persons With Lower-Limb Amputation," *Archives of Physical Medicine and Rehabilitation*, vol. 94, no. 11, pp. 2194–2202, Nov. 2013.

[44] W. C. Miller, A. B. Deathe, and M. Speechley, "Psychometric properties of the Activities-specific Balance Confidence scale among individuals with a lower-limb amputation11No commercial party having a direct financial interest in the results of the research supporting this article has or will confer a benefit upon the author(s) or upon any organization with which the author(s) is/are associated.," *Archives of Physical Medicine and Rehabilitation*, vol. 84, no. 5, pp. 656–661, May 2003.

[45] W. Dite and V. A. Temple, "A clinical test of stepping and change of direction to identify multiple falling older adults," *Archives of Physical Medicine and Rehabilitation*, vol. 83, no. 11, pp. 1566–1571, Nov. 2002.

[46] A. SAWERS and B. J. HAFNER, "NARROWING BEAM-WALKING IS A CLINICALLY FEASIBLE APPROACH FOR ASSESSING BALANCE ABILITY IN LOWER-LIMB PROSTHESIS USERS," *Journal of rehabilitation medicine*, vol. 50, no. 5, pp. 457–464, May 2018.

[47] M. Bellmann, T. M. Köhler, and T. Schmalz, "Comparative biomechanical evaluation of two technologically different microprocessor-controlled prosthetic knee joints in safety-relevant daily-life situations," *Biomedical Engineering / Biomedizinische Technik*, vol. 64, no. 4, pp. 407–420, Aug. 2019, Publisher: De Gruyter.

[48] M. J. Highsmith, J. T. Kahle, S. L. Carey, D. J. Lura, R. V. Dubey, and W. S. Quillen, "Kinetic Differences Using a Power Knee and C-Leg While Sitting Down and Standing Up: A Case Report," *JPO: Journal of Prosthetics and Orthotics*, vol. 22, no. 4, pp. 237–243, Oct. 2010.

[49] A. Seth *et al.*, "OpenSim: Simulating musculoskeletal dynamics and neuromuscular control to study human and animal movement," *PLOS Computational Biology*, vol. 14, no. 7, e1006223, Jul. 2018, Publisher: Public Library of Science.

[50] A. M. Simon *et al.*, "Configuring a powered knee and ankle prosthesis for transfemoral amputees within five specific ambulation modes," *PloS One*, vol. 9, no. 6, e99387, 2014.

[51] A. Simon, N. Fey, K. Ingraham, A. Young, and L. Hargrove, "Powered prosthesis control during walking, sitting, standing, and non-weight bearing activities using neural and mechanical inputs," Nov. 2013, pp. 1174–1177.

[52] H. A. Varol, F. Sup, and M. Goldfarb, "Powered Sit-to-Stand and Assistive Stand-to-Sit Framework for a Powered Transfemoral Prosthesis," *IEEE ... International Conference on Rehabilitation Robotics : [proceedings]*, vol. 5209582, pp. 645–651, 2009.

[53] J. Camargo, A. Ramanathan, N. Csomay-Shanklin, and A. Young, "Automated gap-filling for marker-based biomechanical motion capture data," *Computer Methods in Biomechanics and Biomedical Engineering*, vol. 23, no. 15, pp. 1180–1189, Nov. 2020, Publisher: Taylor & Francis _eprint: https://doi.org/10.1080/10255842.2020.1789971.